AD NUMBER

AD866634

LIMITATION CHANGES

TO:

Approved for public release; distribution is unlimited.

FROM:

Distribution authorized to U.S. Gov't. agencies and their contractors; Critical Technology; JAN 1970. Other requests shall be referred to Air Force Technical Application Center, VELA Seismological Cetner, Washington, DC 20333. This document contains export-controlled technical data.

AUTHORITY

usaf ltr, 25 jan 1972

FREQUENCY DEPENDENT ESTIMATION AND DETECTION FOR SEISMIC ARRAYS

9 January 1970

Prepared For

AIR FORCE TECHNICAL APPLICATIONS CENTER
Washington, D. C.

By

R. H. Shumway
CONSULTANT TO THE SEISMIC DATA LABORATORY

H. L. Husted
SEISMIC DATA LABORATORY

Under
Project VELA UNIFORM

Sponsored By

ADVANCED RESEARCH PROJECTS AGENCY
Nuclear Monitoring Research Office
ARPA Order No. 624

FREQUENCY DEPENDENT ESTIMATION AND DETECTION FOR SEISMIC ARRAYS

SEISMIC DATA LABORATORY REPORT NO. 242

AFTAC Project No.:	VELA T/9706
Project Title:	Seismic Data Laboratory
ARPA Order No.:	624
ARPA Program Code No.:	9F10
Name of Contractor:	TELEDYNE INDUSTRIES, INC.
Contract No.:	F33657-69-C-0913-PZ01
Date of Contract:	2 March 1969
Amount of Contract:	$ 2,000,000
Contract Expiration Date:	1 March 1970
Project Manager:	Royal A. Hartenberger (703) 836-7647

P. O. Box 334, Alexandria, Virginia

DISCLAIMER NOTICE

THIS DOCUMENT IS THE BEST QUALITY AVAILABLE.

COPY FURNISHED CONTAINED A SIGNIFICANT NUMBER OF PAGES WHICH DO NOT REPRODUCE LEGIBLY.

This research was supported by the Advanced Research Projects Agency, Nuclear Monitoring Research Office, under Project VELA-UNIFORM and accomplished under technical direction of the Air Force Technical Applications Center under Contract F33657-69-C-0913-PZ01.

Neither the Advanced Research Projects Agency nor the Air Force Technical Applications Center will be responsible for information contained herein which may have been supplied by other organizations or contractors, and this document is subject to later revision as may be necessary.

TABLE OF CONTENTS

LIST OF FIGURES

LIST OF FIGURES (Cont'd.)

LIST OF FIGURES (Cont'd.)

LIST OF TABLES

ABSTRACT

A frequency dependent detection and estimation procedure based on the generalized likelihood principle is applied to several models appropriate for vertical and horizontal seismic arrays. When data is constructed so as to conform to the idealized model excellent agreement with theoretical detection limits is shown. Multiple signal models are analyzed in the frequency domain with the presence of various signal components indicated in terms of power spectral ratios. Tables of the central and non-central F distribution are used to determine false alarm and signal detection probabilities.

Two models were assumed in analyzing data from vertical arrays. A full model, assuming each time series to be composed of a ghosted signal and an infinite velocity noise component, indicated that in general the infinite velocity component is not present in the "signal plus noise" or the "noise only" cases. A reduced model containing only a ghosted signal plus noise accounted for as much power and produced as good a signal estimate. The signal estimates in general tended to be point by point reproductions of the surface trace indicating that a significant signal to noise enhancement will be difficult using a simple processor. Detection results indicate that in "signal plus noise" cases with a high signal to noise ratio the F statistic exceeds a threshold which would occur by chance much less than one time in 2000. However, "noise alone" analysis also gives a significant (although much less so) value over all frequencies indicating the presence of P waves in the noise. Further analysis on other arrays where the fundamental Rayleigh mode is known to be prominant and where there are lower signal to noise ratios should establish the usefulness of the detector. Analysis of the statistics of the ambient P-noise can also be performed.

For the horizontal array, results using real data indicate that the F statistic, can be a more sensitive detector than the phased sum alone. Examples for the "signal plus noise" case indicate that the signal is detected with a high probability. The "noise alone" analysis yields a low false alarm rate in the particular cases analyzed. Further research can establish the effectiveness of the statistic in determining which frequencies propagate with the signal velocity as well as the level of detection possible with errors in the time delays and sensor calibrations. Models which combine vertical and horizontal arrays are yet to be investigated.

INTRODUCTION

In the analysis of seismic array data a natural extension to the process of estimating a signal by beamforming or deghosting is the development of optimum measures for detecting the presence of certain signals with a given specified probability for a false alarm. Classical procedures involve comparing the peak to peak amplitude of the processed trace to the root mean square of the preceding noise. Such procedures yield reasonable results in that for high signal to noise ratios the signal detection capabilities are often reasonably high. Unfortunately a false alarm probability of .01 for a 50-second sample would not be unusual for such a detector so that the number of false alarms in events per day becomes unacceptably large. Therefore the use of ratios of amplitude to root mean square noise levels must be supplemented by analyst judgement.

It is interesting to note that optimum frequency dependent detectors can be developed in terms of the general likelihood ratio criteria. The optimum detectors involve the comparison of various residual power levels computed under the assumption that various competing signal models are valid. In this report the F detector is developed for signal and noise models which are appropriate for analyzing short period horizontal and vertical arrays. Using simulated data we establish that, for predictable false alarm rates, propagating waves can be detected as a function of frequency with a high level of reliability. When the detectors are applied to real data it is noted that the F statistic can isolate the frequencies moving at the signal velocity more effectively than other measures such as phased sum power spectra. The methods are applied to two events recorded on

a vertical array and to two noise samples from the same vertical array. A single event recorded at the 21 sub-array centers of LASA is analyzed using the theoretical signal model applicable to the horizontal array.

THEORETICAL DISCUSSION

Most signal models arising in seismological applications can be expressed in the general form (see Shumway and Dean [9])

$$Y_j(t) = \sum_{m=1}^{P} \sum_{u=-\infty}^{\infty} X_{jm}(t-u)\beta_m(u) + n_j(t) \qquad (1)$$

$$j = 1, 2, \ldots, N, \quad t = 0, \pm 1, \pm 2, \ldots.$$

The times series $Y_j(t)$ is the recording at jth sensor of a vertical or horizontal array. The jth series $Y_j(t)$ is assumed to be a discrete time stationary process, and is composed of a mixture of signals $\beta_1(u)$, $\beta_2(u), \ldots \beta_p(u)$. The coefficient matrix of time invariant functions $X_{jk}(t)$ is given by specifying a particular model for the signals assumed to be present. The error series $n_j(t)$ are assumed to be uncorrelated from sensor to sensor. The correlation function may have a general form although it is assumed to be identical from sensor to sensor.

In the next sections we will present examples of the various special cases of equation (1) which are relevant to problems in seismological estimation and detection. The approach utilizes finite Fourier transform methods to develop the estimates for the signal and to test the various signal models following the approach described in references [8], [9], and [10].

The Horizontal Array

In particular we may obtain a model for a horizontal

array using equation (1) with $p = 1$, $\beta_1(u) = s(u)$ and $X_{ji}(t) = \delta_{t-T_j}$ where δ_t is the Kronecker delta function defined to be 1 when $t = 0$ and 0 when $t \neq 0$ and $T_1, T_2 \ldots, T_n$ are the time delays defined by the velocity and azimuth of the propagating signal. In this case equation (1) becomes

$$Y_j(t) = s(t-T_j) + n_j(t) \tag{2}$$

and we have the signal model for the horizontal array.

Thus the problem reduces to the detection of a deterministic signal embedded in random noise. If we assume that the signal waveform is known and that $n_j(t)$ is a continuous parameter noise process possessing a Karhunen-Loeve expansion in terms of an infinite set of uncorrelated random variables, an elegant likelihood solution due originally to Grenander [3] is possible. However, the integral equations which must be solved in order to generate the random variables of interest are difficult except for a few simple cases. The assumption that n(t) is a normal white noise process, for example, leads to the well known matched filter (for one example see Selin[7]). Another possible approach can be made via the sampling theorem[7] which also leads to a matched filter detector for the normal white noise case. The difficulties arising in the solution of the integral equations obtained via the likelihood approach to the testing of the hypothesis $s(t) = 0$ in (2) against a specified alternative have led investigators to the use of alternative methods for generating observable test statistics. For example, using Fourier transform methods one can generate random variables which are uncorrelated as the lengths of the time series tend to infinity. In addition, the sample variances of such complex random variables have expected values

equal to the power spectrum if it can be assumed that the time series is wide sense stationary.

In this section we shall consider a general asymptotic solution to the detection problem for a signal model given in the form of equation (2). In particular we consider a frequency dependent likelihood ratio test of the hypothesis that $s(t) = 0$ against the general alternative that $s(t) \neq 0$. The asymptotic distribution of the test criterion is given[10] in terms of the classical F statistic enabling us to set critical threshold values which specify desired false alarm rates. Then, assuming that we have some basic information on the types of alternatives to be tested, a procedure is presented for computing the signal detection probability as a function of the number of time series and the signal power in some frequency band of interest. A number of computational examples verify that the test statistic gives results which are consistent with the predicted false alarm and missed signal rates.

In particular, it has been shown[10] that the maximum likelihood estimator for the signal is the phased sum of the traces and that the likelihood ratio test of the hypothesis $s(t) = 0$ in the frequency domain can be derived from the finite Fourier transforms of the original series $Y_j(t)$ and the likelihood estimates for the signal

$$\bar{Y}(t) = \frac{1}{N} \sum_{j=1}^{N} Y_j(t-T_j). \tag{3}$$

The finite Fourier transform is defined as usual by

$$\tilde{Y}_j(\omega n) = \frac{1}{\sqrt{T}} \sum_{t=0}^{T-1} Y_j(t)\, e^{-i\omega_n t}, \quad \omega_n = \frac{2\pi n}{T}, \quad n=0, 1, \ldots, T-1 \tag{4}$$

with the transforms of $\bar{Y}(t)$ and $s(t)$ given respectively by $\bar{Y}(\omega n)$ and $\tilde{S}(\omega_n)$. In [9] it is shown that an analysis of power given in the form of Table I below yields a likelihood ratio test for the presence of the signal with the components of power following chi-square distributions.

TABLE I

Analysis of Power at Frequency ω_n for Horizontal Array

SOURCE	POWER	DEGREES OF FREEDOM
Due to Signal	$N\lvert\tilde{Y}(\omega_n)\rvert^2$	2
Deviation	$\sum_{j=1}^{N} \lvert\tilde{Y}_j(\omega_n)-\bar{Y}(\omega_n)\rvert^2$	2(N-1)
Total	$\sum_{j=1}^{N} \lvert\tilde{Y}_j(\omega_n)\rvert^2$	2N

We refer to the analysis of the variance involving the complex Hermitian forms in Table 1 as an analysis of power. Now it can be seen from Table I that the power due to the signal is N times the power spectrum of the phased sum of the observed time series whereas the total power is the sum of the power spectra of the original series. Since the test statistic is determined by a monotonic function of the ratio of the power due to the signal to the deviation power, a convenient ratio of two chi-square variates divided by their degress of freedom is

$$F(2,2(N-1)) = \frac{\text{Power Due to Signal}}{\text{Deviation}} (N-1) \qquad (5)$$

which gives a likelihood ratio critical region. The performance of the likelihood detector above is dependent upon the distributional properties of the F statistic in equation (5) under the null and alternative hypothesis. If the hypothesis $s(\omega_n) = 0$ is true then (5) follows a central F distribution so that a specified false alarm rate (Type I error) α determines an upper threshold value for F, say $F_{1-\alpha}(2, 2N-2)$. For a given false alarm rate α the signal detection probability Pd is determined by relative frequency with which the observed F will exceed $F_{1-\alpha}(2, 2N-2)$ where the observed F follows a noncentral F distribution with the noncentrality parameter proportional to

$$\delta^2 = \frac{N|s(\omega_n)|^2}{(\sigma^2(\omega_n)/2} \qquad (6)$$

when the signal is present. Here $\sigma^2(\omega_n)$ is the value of the theoretical noise spectrum at frequency ω_n. If the power of the signal in the frequency band of interest is known as well as the power of the noise, we can compute a value for the noncentrality parameter given in (6). Then, we determine, for a given α, the signal detection probability using the Fox charts for the power of the F test (Scheffe [6], pp 446-455). These charts yield signal detection probabilities for the false alarm probabilities 0.01 and .05 with various values of the noncentrality parameter. Since the noncentrality parameter is determined in terms of the signal to noise ratio, it follows that receiver operating characteristic curves can be computed for the F ratio detector.

In theory, this procedure guarantees a higher signal

detection probability than that which would be obtained by comparing the peak signal amplitude against a long term average noise level. In practice one would prefer false alarm probabilities lower than .01, say .001, which for a 60 second data sample would yield about 1.4 false alarms per day. Hence, for applications, the non central F tables would have to be extended to cover small false alarm probabilities.

The vertical Array

For the vertical array we assume a string of vertically oriented sensors monitoring a signal which progress up the array, is reflected off the top, and then moves back down the array. In the case of Rayleigh and Love waves it is reasonable to assume the presence of a coherent noise trace propagating up the array with an infinite velocity. If we assume that the relative amplitude of the noise varies in a predictable fashion a general model of the vertical array becomes

$$Y_j(t) = \frac{1}{2}\{s(t-T_j) + s(t+T_j)\} + a_j n(t) + n_j(t) \qquad (7)$$

$$j = 1, 2, \ldots N$$

where $T_1, T_2, \ldots T_n$ are the same time delays characterizing the signal at the various sensor locations. Hence, each time series is composed of a fixed noise function n(t) and a signal s(t) which appears as a ghost, first at $t-T_j$, and then at $t + T_j$. Equation (7) can be obtained as a special case of equation (1) by taking P = 2,

$$\beta_1(t) = s(t),\ \beta_2(t) = n(t),\ X_{j1}(t) = \frac{1}{2}\left(\delta_{t-T_j} + \delta_{t+T_j}\right)$$

and $X_{j2}(t) = a_j\ \delta_t$ where δ_t is the Kronecker delta as before. The a_j are constants which may be thought of as the amplitude of a Rayleigh mode at a particular frequency.

In the multiple signal of signal-coherent noise model specified by (7) a reasonable sequence of tests of hypotheses might be given by

$$H_1: n(t) = 0$$
$$H_2: s(t) = 0 \text{ given } n(t) \neq 0 \qquad (8)$$

The above procedure tests first to see if there is an infinite velocity coherent noise trace present. If the hypothesis $n(t) = 0$ is rejected (the usual case) the processor tests the hypothesis that with coherent noise present there is no signal propagating up the array with a finite velocity described by the time delays given in (8). In [8] it is shown that a sequence of likelihood ratio tests in the form (8) yields the analysis of power table given below where the exact expressions for the power components are more complicated.

TABLE II

Analysis of Power at Frequency ω_n for a vertical array

Source	Power Symbol	Degrees of Freedom
Due to Coherent Noise	P_{nn}	2
Difference (a)	Diff(a)	2
Due to Signal and Coherent Noise	P_{ss+nn}	4
Due to Incoherent Noise	P_{ee}	2(N-2)
Total Power	$P_{ss+nn+ee}$	2N

The statistic for testing for coherent noise is

$$F(2,\ 2N-2) = (N-1)\ \frac{P_{nn}}{(Diff(a) + Pee)} \tag{9}$$

which has the F distribution with 2 and 2N-2 degrees of freedom. A statistic for testing for the signal is given by

$$F(2,\ 2N-4) = \frac{Diff(a)}{P_{ee}}\ (N-2) \tag{10}$$

which has the F distribution with 2 and 2N-4 degrees of freedom.

For this case the false alarm rate may be specified as α by using $F_{1-\alpha}(2,2(N-2))$ as a threshold value to be exceeded only 100α percent of the time when there is no signal present.

The above detection procedure yields as residual results asymptotically best linear unbiased estimates for the signal s(t) and the coherent noise n(t). The estimates are also asymptotic maximum likelihood estimates. By asymptotic we mean that the properties hold with T large where T is the number of data points.

The next section presents several simulated examples designed to illustrate the estimation procedure and to verify the performance of the F statistic as an optimum detector.

SIMULATED EXAMPLES

In order to determine whether or not the finite versions of the previously discussed asymptotically optimum procedures give reasonable results, a number of test cases were run using simulated horizontal and vertical array data. The results are presented in the following two sections.

A Simulated Horizontal Array

In order to illustrate the preceding sections it is necessary to generate sets of time series conforming to the signal plus noise model specified in equation (3). A 128 point test signal of the general form

$$s(t) = \alpha t\, e^{-\alpha t} \sin \beta t,\ t = 0,1,\ldots,127 \qquad (11)$$

was generated where, as a frame of reference, it is assumed that the data are obtained at a sampling rate of 20 points

per second. Hence the frequency range covered runs from 0 to 10 cycles per second (cps). Figure 1 shows a 128 point two cycle per second signal generated according to (11). This signal is to be buried at differing magnitudes in a 1024 point multivariate stationary noise process. Two types of noise processes were used in the simulation, white Gaussian (normal, independent, zero mean) noise with unit power density at all frequencies and a smoothed white noise process with smoothing coefficients .10, .20, .-10, .20, .50 and -.10. An estimate for the power spectrum of the smoothed series is shown as the total power component in Figure 7. Figure 2 shows a typical portion of a 1024 point smoothed white noise series containing a test signal whose maximum amplitude is 0.5. The double arrow specifies the entry point of the signal. For the first example ten series were generated with each of the two types of noise structures and with maximum signal amplitudes of 0.0, 0.5, and 1.0 respectively. Figure 3 shows the mean value of ten processes of the same type as that shown in Figure 2 and we see that there is in the averaged trace some indication of a signal. A detector based on signal amplitude alone would obviously produce a number of false alarms. Figures 4, 5, and 6 summarize the analysis of power and F tests for the maximum signal amplitude levels of 0.0, 0.5, and 1.0 respectively when the signals are buried in white Gaussian noise with a unit spectrum. For practical applications it is desirable to smooth the spectral estimates over bands of approximately constant spectral power. This increases the degrees of freedom for the estimates and reduces the volume of data for display. In effect this modifies Table I in that if the power component for a single n is distributed as $\frac{\sigma^2(\omega n)}{2} X^2_{2N}$ then the average of k identical independent spectral estimates would be $\frac{\sigma^2(\omega_n) X^2_{2Nk}}{2k}$ so that entry should

be divided by N and compared with a $\frac{X^2_{2Nk}}{2Nk}$ to verify the theoretical distribution. Therefore for $\sigma^2(\omega_n) = 1$ as in Figures 4, 5, 6 a multiplier of 2 has already been divided out in the smoothing procedure so that the observed chi-square variables in the figures appear to have only have as many (2,8 and 10) degrees of freedom as would be indicated from Table I. The number of time series, N, is ten for this particular example. In this set of figures 33 estimates of the power spectrum are made and each estimate is an average of 17 adjacent values yielding 2 X 17 = 34 degrees of freedom for the signal power and 2 x (10 - 1) x 17 = 306 degrees of freedom for the error power. If the false alarm rate is set at $\alpha = .05$, we use $F_{.95}(30,300) = 1.46$ as the critical threshold. As the amplitude of the signal is increased we may note the improving capability of the detector. When the analysis is repeated using smoothed white noise (Figures 7,8 and 9) we observe similar improvements in the detector performance. Table III below summarizes some parameters of interest for this first example involving ten 1024 point time series.

TABLE III

Parameters of Interest for 10 Time Series
Each Containing a 128 Point Signal

Identification	Signal Amplitude	Maximum Signal Power (2.0 cps)	Noise Power (2cps)	Non Centrality Parameter	* α	** 1-β
Figure 5 White Noise	0.5	.086	1.00	.9	.05	.8
Figure 6 White Noise	1.0	.343	1.00	1.9	.01	.99
Figure 8 Smoothed White Noise	0.5	.086	.55	1.3	.01	.9
Figure 9 Smoothed White Noise	1.0	.343	.55	2.5	<.01	>.99

*α = Specified False alarm probability

**1 - β = Pα = Theoretical signal detection probability from the Fox tables for the power of the F test.

The maximum signal power (in equation (6)) is evaluated by computing the average power over the same interval as the spectral estimates on the basis of 1024 points. The theoretical detection probability P_d is computed using the Fox tables [6]. It is apparent from Figures 4 - 9 that, for a variety of signals, a frequency by frequency detector based on spectral power computations and the F statistic gives results consistent with theory.

However, if the procedure is to be applicable to a broad range of problems the theoretical false alarm and signal detection probabilities ought to match the results of simulation experiments. In order to examine the performance measures over a larger number of trials and for a limited number of degrees of freedom a number of simulated runs involving only three time

series were made over the parameter ranges specified in Table IV below. In this case 65 estimates of the power spectrum are generated where each spectral estimate is an average of 9 adjacent estimates yielding 18 degrees of freedom for the signal power and 18 x (3-1) = 36 degrees of freedom for the error spectrum. The noise power at 2 cps is .55.

TABLE IV
Theoretical Parameters for Simulation
(Two Cycle per Second Signal Buried in Smoothed White Noise, N = 3)

Identification	Signal Amplitude	Maximum Signal Power (2cps)	Non Centrality Parameter (2 cps)	α	$1-\beta$
A	0.50	.145	.9	.05	.5
B	0.75	.327	1.3	.01	.7
C	1.00	.582	1.8	.01	> .9

A number of repetitions of each of experiments, A, B, and C in Table IV above yielded the sample performance characteristics shown in Table V. Sample false alarm probabilities were estimated by counting the false alarms in the frequency bands outside the 2 cps range.

TABLE V
Sample Error Rates and Signal Detection Probabilities
For Simulated Data

Identification	Number of Signals	Number of Signals Detected	Sample False Alarm Rate	Sample Signal Detection Probability
A	34	15	.04	.44
B	38	29	.01	.76
C	36	35	.01	.97

Again the sample results compare favorably with theoretical values predicted from Table IV.

A practical procedure then is suggested which is similar to the usual analysis of variance approach. First one decides on the frequency resolution desired for the analysis of power. This determines, with a fixed data length, the number of spectral estimates and the number of degrees of freedom for each spectral estimate. As an alternative hypothesis one then chooses a class of signals of length L say with a certain waveform which are to be detected with certain probability for a given false alarm rate. The noncentrality parameter for the F detector as a function of frequency is determined by appending T - L + 1 zeros to the signal and then computing the smoothed spectrum in the same fashion as for the smoothed estimates in the analysis of power. For a given false alarm rate the number of data series (sensors) required to detect the signal with a given probability can be estimated. If the number of time series is fixed then degrees of freedom and hence the signal detection level can be adjusted by increasing the length of the data series or by cutting down the number of spectral estimates involved in each smoothed estimate.

A Simulated Vertical Array

Ten time series containing 1024 points each were generated according to the model specified by (7). In order to provide a check on the probability distributions involved in the analysis of power the errors $n_j(t)$ were taken as normal independent random variables with mean zero and unit variance. Under this convention one would expect the spectra of the error traces to be unity for all frequencies. A fixed coherent noise function n(t) to be added to each trace was generated by taking three point running averages of zero mean independent normal random variables. This generates a series with a predictable power

spectrum. A portion of the 1024 point fixed function n(t) is shown in Figure 14 and its theoretical spectrum is given in Figure 16. An arbitrary sampling rate of 20 points per second is assumed which yields a ten cycle per second folding frequency corresponding to the point π. The signal s(t) is generated as a relatively short (128 point) exponentially decaying sine wave oscillating at three cycles per second, and is shown in Figure 12. Figure 10 shows a 240 point portion of one of the ten time series simulated according to the model implied by (7) with $a_1=a_2=\ldots=a_{10}=1$. The maximum amplitude of the signal function is 4.0 while the coherent noise and random error have unit variance each. The arrows signal the two entry points for s(t) and are respectively 23 points to the left and right of the center point.

Now for the vertical array model (7) with $a_j=1$ we may write $X_{j1}(t) = \frac{1}{2}[\delta_{t-T_j} + \delta_{t+T_j}]$ where δ_t is 1 when $t=0$ and 0 otherwise. Then we may write the Fourier transform of $X_{j1}(t)$ as

$$\tilde{X}_{j1}(\omega) = \sum_t [\delta_{t-T_j} + \delta_{t+T_j}] e^{-i\omega t} = \cos \omega T_j \qquad (12)$$

with $\tilde{X}_{j2}(\omega) = 1$ so that the solutions for the best linear unbiased filters in frequency may be written using the usual matrix equation [9].

$$H(\omega) = (X^*X)^{-1} X^*(\omega) \qquad (13)$$

for the optimum filters at each frequency. This determines

$$\tilde{H}_{1k}(\omega) = \frac{1}{\Delta(\omega)} [N \cos\omega T_k - B(\omega)] \qquad (14)$$

$$\tilde{H}_{2k}(\omega) = \frac{1}{\Delta(\omega)} [A(\omega) - B(\omega) \cos \omega T_k] \qquad (15)$$

with

$$A(\omega) = \sum_{k=1}^{N} \cos^2 \omega T_k, \quad B(\omega) = \sum_{k=1}^{N} \cos \omega T_k, \quad \Delta(\omega) = NA(\omega) - B^2(\omega) \tag{16}$$

where k=1,...,N. In theory the frequency functions (14) - (16) could be multiplied and summed frequency by frequency with the transforms of the original time series in the frequency domain version of a matrix convolution. In practice, we avoid end effects and simulate the infinite two sided nature of the convolution by constructing the time functions $h_{jk}(t)$ over a shorter time interval than the interval over which the original time series $y_j(t)$ are known. The interval of length L say must be long enough to cover the largest time delays specified by the linear model and short enough to avoid the end effects inherent in finite convolutions. Then we may compute the frequency functions at each of the frequencies $\omega_j = 2\pi_j/L$, j = 0, 1,...,L-1. The complication at $\Delta(0) = 0$ is eliminated by assigning $H_{jk}(0) = 0$ so that the filters do not pass the zero frequency. The finite Fourier transform applied to the frequency functions (14) - (16) yielded the time functions shown in Figure 11 for N - 10 and L = 128 points. The filter for estimating the mean effect contains the expected peak at time zero for all $h_{1k}(t)$. The signal estimation, or s(t) filters, contain the peaks at the time delays at which the signal appears. For the tenth series the time delay was 23 points. The negative small peaks match the signal time delays at the other levels. Hence we have a matrix of filters reminiscent of the adjusted row and column totals which estimate effects in the classical analysis of variance. Now the 128 point filters may be extended by adding zeros and convolved with the multivariate time series ($Y_k(t)$, k = 1,...,10, t=1,...,1024) using the usual finite Fourier transform approach.

The true and estimated signals are shown in Figure 12 and Figure 13. Portions of the true and estimated noise functions are shown in Figure 14 and Figure 15 respectively. The portion of the estimated signal shown is a segment which was originally confounded with the noise function on the original traces and it can be seen that both estimates are remarkable repr ductions of their known signatures. It is of interest to point out that the method of estimation is independent of any postulated waveform for either the signal or the noise.

For the linear model presented here we are interested in the following sequence of tests,

H_1: $n(t) = 0$

H_2: $s(t) = 0$ given $n(t) \neq 0$

This is seen to be an example of a sequence of tests of the kind given in Table II. As a practical matter the power due to n(t) is seen to be the power spectrum of the predicted trace Y(t) under the assumption that $s(t) = 0$.

Thus the power due to the mean is $N|\bar{Y}(\omega)|^2$ which is computed from the mean value of the time functions by the usual finite Fourier transform methods. Similarly it can be seen that the power due to fitting both n(t) and s(t) quoted as P_{ss+nn} in Table III is just the sum of the power spectra of the predicted time series when neither n(t) or s(t) are zero. This term could be computed directly in the frequency domain but is more easily computed by constructing the predicted series at each level under the assumption that neither s(t) nor n(t) are zero and then summing the power spectra of these predicted series computed by the usual finite Fourier transform methods. The total power is obtained by summation of the power spectra of each of the original time series. Other terms are obtained by differencing.

Figures 17, 18 and 19 summarize the analysis of power results. In Figure 17 we observe the three successive power components as a function of frequency. In general the computational procedure for a power component here was to compute 31 point running averages of the squared finite Fourier transforms of the original 1024 point time series. This yielded 33 power spectral estimates with approximately 60 degrees of freedom each. Adjacent estimates are slightly correlated. In Figure 17 the power due to the noise plus signal function shown as the solid line contains the expected peak at 3 cycles per second, the frequency of the signal function s(t). The difference between the total power and the power due to s(t) is uniform at all frequencies as is expected since the input error trace has a constant power spectrum. Figure 18 shows the F statistic for testing the noise function computed from Equation (10). The degrees of freedom are then because of the smoothing approximately $31x2x1 \approx 60$ and $31x2(10-2) \approx 500$. Since the error spectrum is again uniform the F statistic as a function of frequency approximates the spectrum given in Figure 16. Obviously coherent noise is present. Figure 19 shows the F statistic computed using Equation (10) for testing the signal function and we see the expected highly significant peak at the signal frequency of 3 cycles per second. At other frequencies the statistic stays below its critical value. Thus when the signal is present even as a 128 point function buried in a 1024 point series the F ratio statistic is a highly sensitive detector.

In order to examine the analysis of power when the signal was not present the entire procedure was repeated with data simulated according to the signal free model. Again the error power has a uniform spectrum with the appropriate degrees of freedom, and the F statistic for testing the significance of

the signal function s(t) conforms well to its null F distribution with 60 to 500 degrees of freedom. Of course, the F statistic for testing the noise function n(t) still remains significant. Finally the analysis of power was repeated on simulated data containing only the error process $e_j(t)$. This time neither of the F statistics are more than occasionally significant and they both conformed approximately to the null distributions.

SEISMIC ARRAY DATA

In the previous sections we have established that for data conforming to one of the two basic models, the detection and estimation procedure presented in Section 2 is effective. The excellent agreement between the theory and the results of the simulation confirms the correctness of the computer programs and the validity of the asymptotic approximations used. The next logical step is to examine the performance of the optimum detector on a reasonable test set of seismic data. For this purpose a horizontal array composed of 21 subarray centers at LASA and a representative short period vertical array of recording instruments including the surface was chosen.

Horizontal Array

A representative event at the 21 subarray centers for LASA is shown for several sensors in Figure 20. An analysis of power (see Table I) for this event yielded the power components shown in Figures 21 and 22. The power spectrum of the beam formed sum shows significant power components at .5 and 1.0 cps. However the F statistic indicates that the signal model implied by the beam is only significant at .5 cps as can be deduced from Figure 23. Hence the power at 1

cps is not explained by the signal model and may be due either to site reverberations or signal generated noise. The power due to the unexplained noise (Figure 22) also shows a strong contribution at 1 cps. In order to check the performance of the F statistic on noise the analysis was repeated when the signal was absent. The result shown in Figures 24 - 26 indicate that at a reasonable threshold no false alarms were observed for this particular case.

The processor is useful not only as an improved automatic detector but can isolate frequencies which are not propagating with the beam characteristics. It is fairly simple to extend the results to the case where more than the signal is present as, for example, to the model

$$Y_j(t) = s_1(t-T_j) + s_2(t-D_j) + e_j(t). \qquad (17)$$

The estimation of both signals has been considered (see [9]) and the detection theory can be developed for testing whether one or both of the signals is present at a given frequency. Hence the procedure will discriminate on a frequency by frequency basis between signals from different sources or detect the presence of directional noise. The sensitivity of the F statistic as a means for resolving signals from different directions is yet to be investigated.

Vertical Array

Previous investigations of the vertical array using the likelihood filters and the plane parallel layering Rayleigh noise model as described in Dean [2] have not been effective. It was established that for simulated data Rayleigh Wave rejection by optimum filtering would be possible. This section describes some further experimental results using two simplified models along with the F statistic as a diagnostic model indicator.

For the data analysis, a short period vertical array (site 207) recorded an event from the Fiji Islands and an event from the east coast of Colombia. Time delays, read from the records (see Equation (7)) were .00, .12, .21, .28, .36, .43, and .52 seconds respectively. These are one way travel times read starting at the surface.

All data are prepared by a bandpass filter operating over the band (.6-2.0) cycles per second. Figure 28 shows the basic data used as input to the optimum processor program. A visual examination of the various recorded outputs indicates that the noise preceding the signal might conform reasonably well to the noise model given in (7) and for reference we reproduce the basic vertical array model to be considered as

$$Y_j(t) = \tfrac{1}{2}\{ s(t-T_j) + s(t + T_j)\} + a_j n(t) + \epsilon_j(t) \qquad (18)$$

$$j = 1,\ldots,7$$

The noise preceding the signal appears to have the same waveform from level to level except for the amplification factor a_j, but it is difficult to determine the velocity of propagation which may be close to that of the signal. The relative amplification factors were estimated by examining a noise record preceding the signal. The relative amplitudes of the apparent infinite velocity noise were read for each event and were not assumed to vary over the frequency range of the data. The a_j's did not in general attenuate with depth as would be expected if n(t) were fundamental mode Rayleigh noise. A typical section of noise record is shown in Figure 30 for 14007 and again we notice the high coherence between the sensor outputs. If a separation between the signal and noise propagation modes is possible then the analysis of power given in Table II should show separate components due to the signal and coherent noise.

In order to apply the technique described in the previous sections . to the preceding vertical array data the filters given in Equations (14), (15), and (16) were generated in frequency and the results were transformed to the time domain. One of the resulting filters in frequency and time is shown in Figure 27 for both the signal estimator and the noise estimator. The signal estimation filters in time contain the expected peaks at the positive and negative time delays with a negative noise suppression peak in the center.

When the optimum filters were applied to the vertical arrays with the signal present, the filtered outputs (Figures 29 and 33) give an almost identical reproduction of the signal as it appears at the surface. Since the noise level (compared to the surface) is not reduced appreciably on the filtered output, there appears to be significant noise propagating with the signal velocity. The estimated noise traces (Figures 29 and 33) indicate signal generated noise in the case of Figure 29 but not as much signal generated noise in the case of Figure 33. If the filters are convolved with a set of outputs containing noise alone (Figure 31), both filtered outputs look similar to the apparent common noise trace as can be observed from Figure 30. This indicates that significant energy in the noise may be propagating at both P wave and Rayleigh velocities.

In order to examine the apparent difficulty of the filters in separating the signal velocity and noise velocity components, it is interesting to look at the detector results as read from the analysis of power given by using Table II. For the analysis of power computations the following parameters and conventions are used. The sampling rate is approximately 40 points per second yielding a folding frequency of 20 cycles. Estimates are generated from 2048 data points with the spectral estimates composed by taking 15 point running averages which yielded

15x2 or 30 degrees of freedom per spectral estimate. With 7 data series the degrees of freedom for the error spectrum are (7-2)x15x2 = 150 so that the appropriate F statistic has 30 and 150 degrees of freedom.

Table VII shows the analysis of power results on the Fiji Island event when the full model given by Equation (18) is applied. In this first case, the signal is present (Figure 28) and the F statistic for detecting the signal is appropriately significant over the whole range at the 1% level. The maximum value for the total power component, computed by summing the individual original power spectra, occurs at .8 cps whereas the maximum of the F statistic for detecting the signal is closer to the usual signal frequency (1.4-1.6 cps). We notice here that the F statistic for detecting coherent infinite velocity noise exceeds the critical level only at a very low frequency (.4 cps) implying that we reject the hypothesis that such a coherent noise signature is present except at low frequencies. It will be noticed that in the lower frequencies the power components are not always additive so that F values become large or are negative. These F values are included in the Tables for completeness but should not be relied upon as indicators for the presence of signal or noise at low frequencies. The reason for the non additivity lies in the restriction that the filters not pass Love frequency. Hence, for 128 point filters, the frequency response is incorrect from 0 to .16 cps. Now the spectral averages are computed by 15 point running averages which lead to a bandwidth of approximately 13 cps. Hence an estimate centered at .6 cps is about the lower limit of credibility for the power components and F ratios. Lower frequencies can be examined by decimating the data and taking a longer time series. To verify that the infinite velocity noise form does not describe the data adequately, a section of

data immediately preceding the Fiji Island signal was analyzed in a "noise-alone case". The analysis of power (Table VII) shows again that the "signal-like noise" dominates the noise which might be propagating with infinite velocity. The F statistic indicates at a high significance level that a signal is present or that a time trace with a signal velocity can be isolated. And also, that infinite velocity noise is present. In Table VIII a Colombian event is analyzed and the results are similar to the Fiji Island case. The F statistic for detecting the signal is highly significant at 1.6 cps with the noise F ratio only occasionally significant.

Since the noise propagating at infinite velocity was generally not significant, we may consider a reduced version of (18) given by

$$Y_j(t) = \tfrac{1}{2}\{s(t-T_j) + s(t+T_j)\} + n_j(t) \qquad (19)$$

which does not include a coherent noise component. The results, shown in Figures 34 - 36 tend to confirm that the optimum filters for the reduced model produce an adequate version for the estimated signal. The analysis of power using the reduced model (19) is shown in Table IX and we see that the assignment of the coherent noise power term to the error spectrum has not adversely affected the power due to the signal. By comparing, for example, the frequency band centered at 1.4 cps for Table IX with the corresponding entries in Table VI we see that the error power (39.52 - 30.19 = 9.33) increases to 12.59 reflecting some of the coherent noise moving into the incoherent error spectrum.

The F statistic for detecting the signal continues to be highly significant in the signal band (1.4 - 1.6 cps). In the signal free case (Table X) the noise propagating with a signal-like velocity again gives a significant number of false alarms using the F statistic. However, the magnitudes of the observed

TABLE VI

Analysis of Power for Fiji Island Event (Full Model, Signal Only)

Frequency cps	.4	.6	.8	1.0	1.2	1.4	1.6	1.8	2.0
P_{nn}	9.59	18.70	25.84	7.87	15.96	4.90	.27	.07	.06
P_{nn+ss}	18.14	71.09	130.11	76.52	75.11	30.19	3.96	.30	.13
Total	12.62	87.18	181.82	144.16	147.16	39.52	5.32	.52	.30
F(Coherent Noise)	1.89	1.64	.99	.35	.95	.85	.32	.90	1.32
F(Signal)	--	--	10.11	5.07	7.03	13.56	13.56	5.40	2.07

$F_{.001} = 2.26$

TABLE VII

Analysis of Power for Fiji Island Event (Full Model, Noise Only)

Frequency cps	.4	.6	.8	1.0	1.2	1.4	1.6	1.8	2.0
P_{nn}	1.79	1.74	1.05	.34	.12	.01	.01	.02	.04
P_{nn+ss}	2.80	3.27	2.75	.88	.26	.05	.02	.03	.10
Total	2.24	3.71	3.67	1.46	.39	.09	.04	.07	.30
F(Noise)	23.92	5.26	2.39	1.81	2.67	1.18	1.38	1.90	.83
F(Signal)	--	17.10	9.33	4.70	5.27	3.86	5.93	2.26	1.41

$F_{.001} = 2.26$

TABLE VIII

Analysis of Power for Colombian Event (Full Model, Signal Present)

Frequency cps	.4	.6	.8	1.0	1.2	1.4	1.6	1.8	2.0
P_{nn}	*4.09	2.63	1.32	2.44	1.10	.98	.21	.26	.15
P_{nn+ss}	*5.60	6.57	5.55	8.10	6.63	6.38	3.78	3.14	.50
Total	*4.89	7.21	8.03	12.98	10.82	8.61	6.52	5.28	1.26
F(Noise)	30.71	8.30	1.18	1.39	.68	.77	.40	.32	.81
F(Signal)	--	30.98	8.54	5.80	6.60	12.10	19.90	6.73	2.32

$F_{.001} = 2.26$

TABLE IX

Analysis of Power for Fiji Island Event (Reduced Model, Signal Only)

Frequency cps	.4	.6	.8	1.0	1.2	1.4	1.6	1.8	2.0
P_{ss}	4.46	35.11	79.35	80.09	57.25	26.93	3.82	.26	.10
P_{ee}	8.15	52.01	102.47	84.15	59.91	12.59	1.50	.26	.20
Total	12.62	87.18	181.82	144.16	117.16	39.52	5.32	.52	.30
F(Signal)	3.29	4.06	4.65	4.28	5.73	12.83	15.28	5.82	3.03

$F_{.001} = 2.26$

F ratios are considerably lower than in the case where the signal is present and offer a reasonable basis for deciding whether a signal is present. The fact that there is very little power in the signal band for Table X suggests that we are detecting very weak P arrivals which are apparently always present. The analysis of power for the Colombian event (Table XI) shows similar results and can be compared with the analysis given in Table VIII.

The above experimental results tend to indicate that the reason for the unimpressive filtering results is the presence of significant noise which propagates within the signal band at the same velocity as the signal. This phenomenon can be examined by a frequency wave number analysis of the noise alone and the signal plus noise cases. Figures 37 and 38 show the frequency wave number spectra for data on the Fiji Island event limited to the frequency band 1-2 cps and we may note again the almost identical velocity characteristics of the noise and the signal.

DISCUSSION

In this study of optimum estimation and detection procedures for seismic arrays it was established that when theoretical models postulated for vertical or horizontal arrays hold (as in the simulated examples in Section 3) the methods will perform as advertised. The construction of intuitively pleasing power ratios as F detectors and frequency dependent maximum likelihood estimation procedures present few computational problems.

An example showed that the horizontal array detector can aid in the model specification problem by isolating signals from identical or different sources. We also were able to give an optimum statistic for detecting the signal, expressed in

TABLE X

Analysis of Power for Fiji Island (Reduced Model, Noise Only)

Frequency cps	.4	.6	.8	1.0	1.2	1.4	1.6	1.8	2.0
P_{ss}	.67	1.05	1.37	.61	.17	.04	.02	.01	.06
P_{ee}	1.58	2.67	2.30	.85	.23	.05	.02	.05	.25
Total	2.24	3.72	3.67	1.46	.40	.09	.04	.06	.31
F(Signal)	2.53	2.36	3.58	4.34	4.36	3.92	6.05	1.47	1.38

$F_{.001} = 2.26$

TABLE XI

Analysis of Power for Colombian Event (Reduced Model, Signal Only)

Frequency cps	.4	.6	.8	1.0	1.2	1.4	1.6	1.8	2.0
P_{ss}	*1.34	2.53	3.22	5.40	5.26	5.80	4.97	2.93	.47
P_{ee}	*3.54	4.68	4.80	7.58	5.56	2.81	1.54	2.36	.79
Total	*4.89	7.21	8.03	12.98	10.82	8.61	6.52	5.28	1.26
F(Signal)	2.27	3.24	4.03	4.27	7.17	12.38	19.27	7.44	3.60

$F_{.001} \approx 2.26$

*Each entry should be multiplied by 10^{-5}

terms of the individual spectra and the phased sum spectrum. Using this detector one can set an arbitrary false alarm probability which determines a signal detection probability in terms of the signal power divided by the noise power. An event recorded at 21 LASA subarray centers gave reasonable results.

A basic difficulty in the application of the likelihood estimation procedure to the vertical array was that P wave noise was present which interfered with the estimated signal waveform. This interference combined with the degradation of the signal waveform down the array kept the signal to noise ratio of the processed trace about the same as the surface trace. However, the vertical array shows promise as a detector even in the presence of interfering P noise. The F statistic shows some stability for the "noise alone" case for the two events analyzed and exceeds a very high threshold when the signal is present. The failure of F to follow its exact theoretical signal free distribution when noise only is present need not indicate that the detection procedure will fail. One may measure the F associated with ambient P noise to establish a null non central F distribution. If the F statistic computed for the signal present case exceeds its threshold consistently even for low signal amplitudes the detector can still perform consistently. This is presently under investigation as well as are efforts to realistically model the ambient noise.

In summary, we have shown that the generalized likelihood ratio approach can solve simultaneously the detection and estimation problems on a frequency by frequency basis. A very general model can be used which includes many multiple signal, multiple noise propagation modes as special cases. The procedure is general enough to be applicable to horizontal arrays, vertical arrays, or combinations of horizontal and vertical

arrays. A major application of the generalized theory presented is the testing of one postulated theoretical model against another. In this way the analysis of power aids in the important task of model specification using reasonable statistical testing procedures.

REFERENCES

[1] Bendat, J.S. and Piersol, (1966), Measurement and Analysis of Random Data, Wiley.

[2] Dean, W.C., (1966), Rayleigh Wave Rejection by Optimum Filtering of Vertical Arrays. Seismic Data Laboratory Report No. 166, Teledyne, Inc.

[3] Grenander, U., (1950), Stochastic Processes and Statistical Inference, Ark. for Mat., Vol. 1, No. 17, p. 195.

[4] Parzen, E., (1967), Time series Analysis for Models of Signal Plus White Noise, in Spectral Analysis of Time Series, edited by B. Harris, Wiley.

[5] Rao, C.R., (1968), Linear Statistical Inference and its Applications, Wiley.

[6] Scheffe, H., (1959), The Analysis of Variance, Wiley.

[7] Selin, I., (1965), Detection Theory, Princeton University Press.

[8] Shumway, R.H., (1969), Regression and Analysis of Variance for Multivariate Time Series, Submitted.

[9] Shumway, R.H., and W.C. Dean, (1968), Best Linear Unbiased Estimation for multivariate Stationary Processes Technometrics 16, 523-534.

[10] Snumway, R.H., (1969), Applications to Signal Detection of an Asymptotic Version of Hotelling's T^2, Submitted.

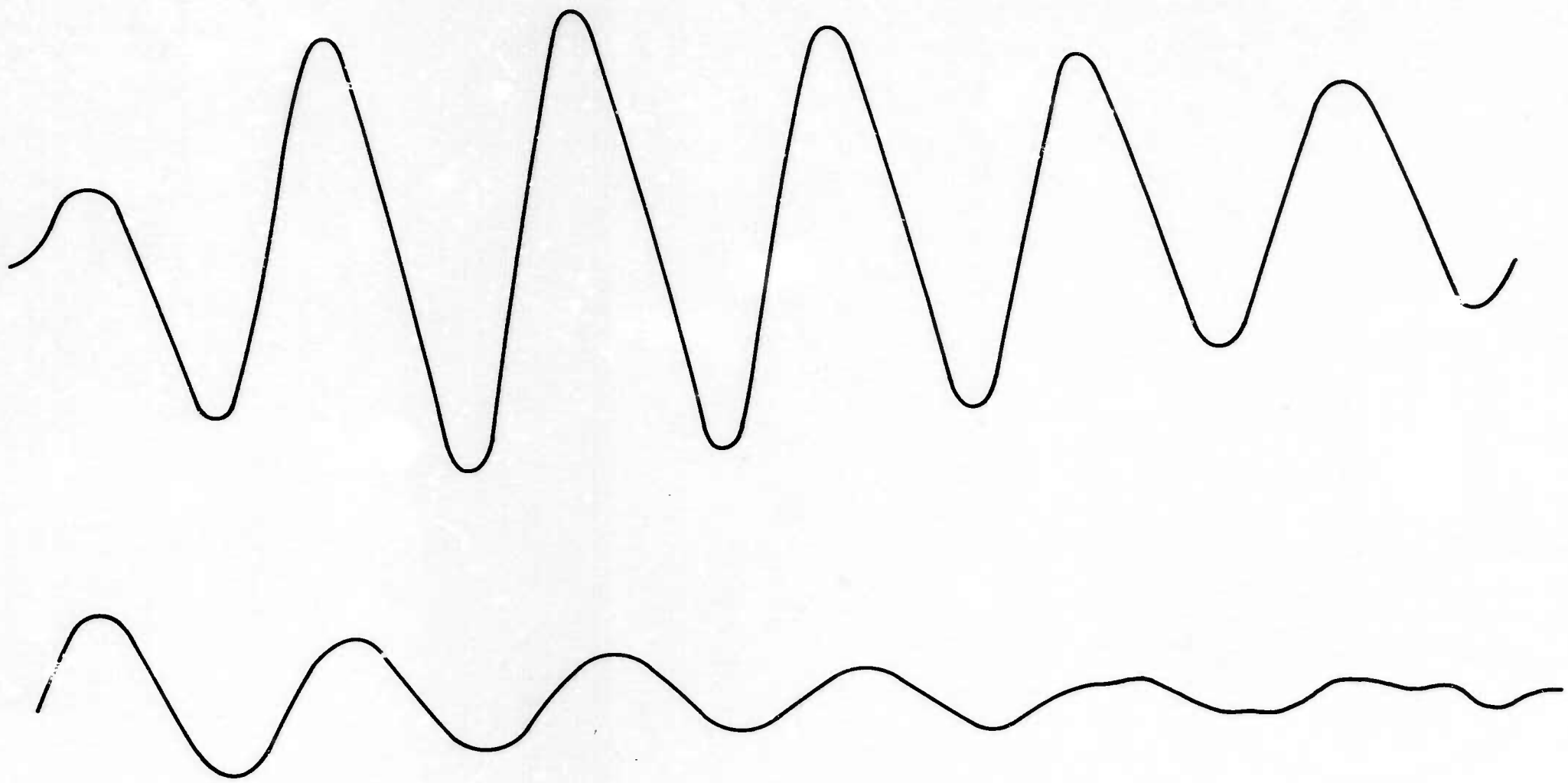

Figure 1. Two cycle per second exponentially decaying sine wave test signal.

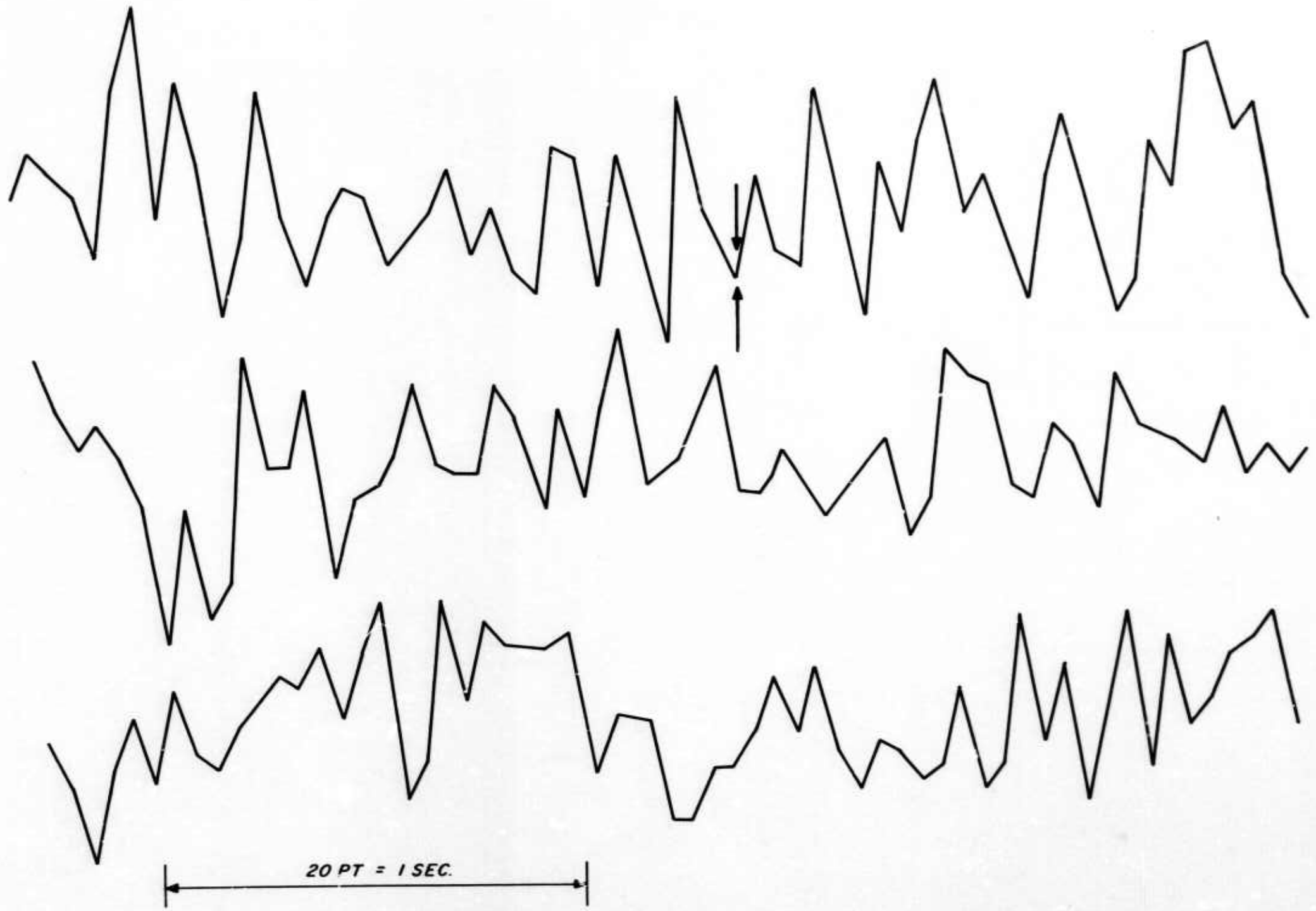

Figure 2. Test signal of amplitude .5 immersed in smoothed white noise with average root mean square = 0.6 in signal band.

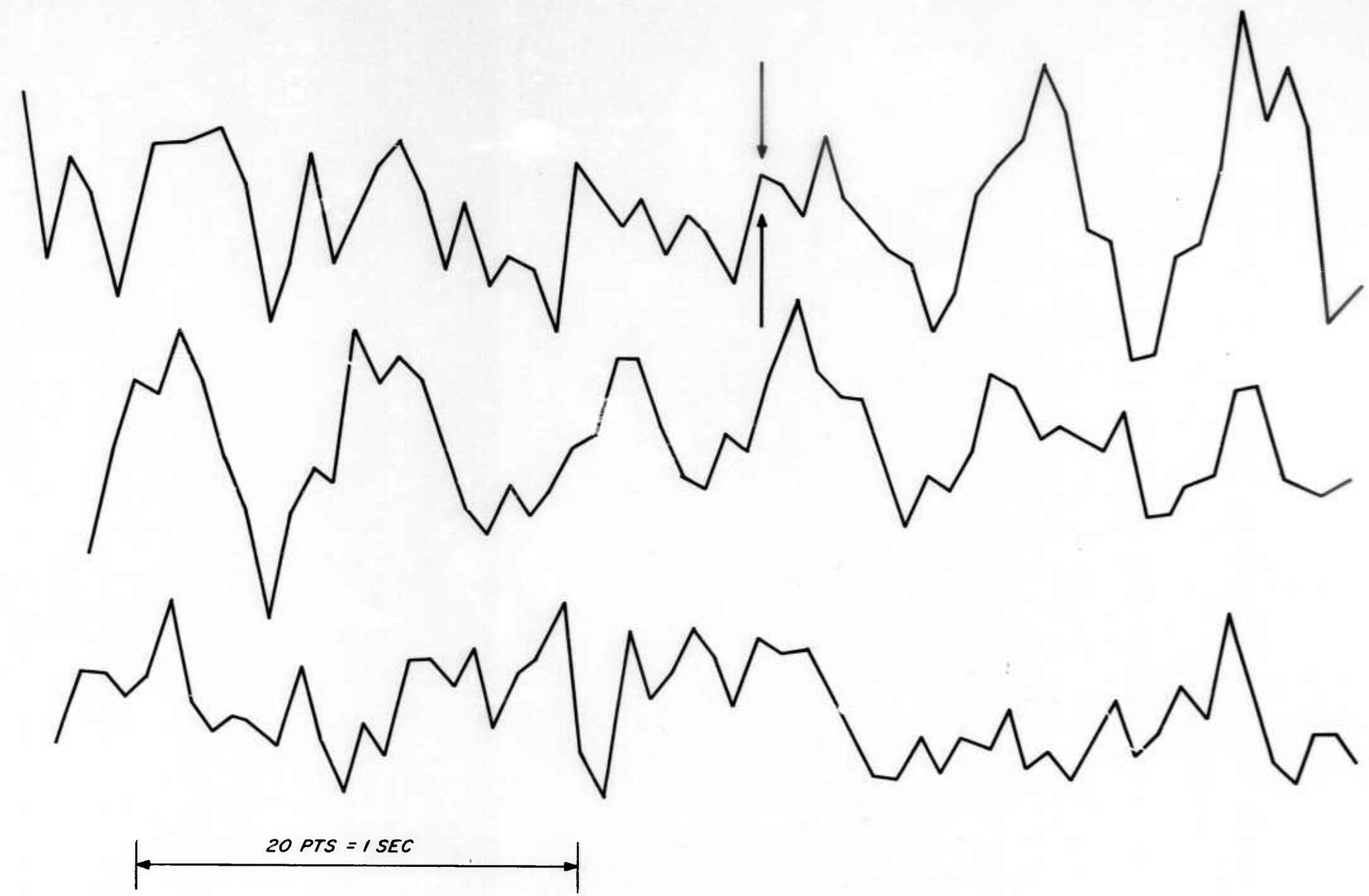

Figure 3. Mean value of ten processes of the type displayed in Figure 2.

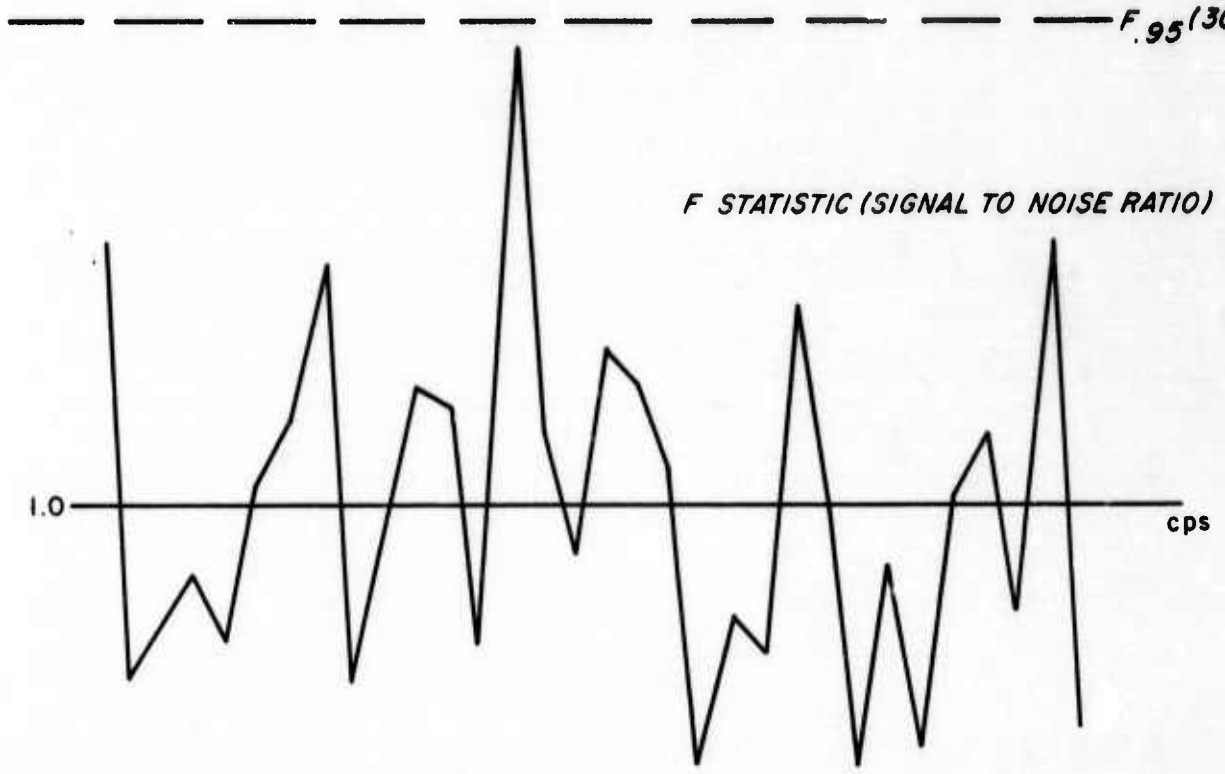

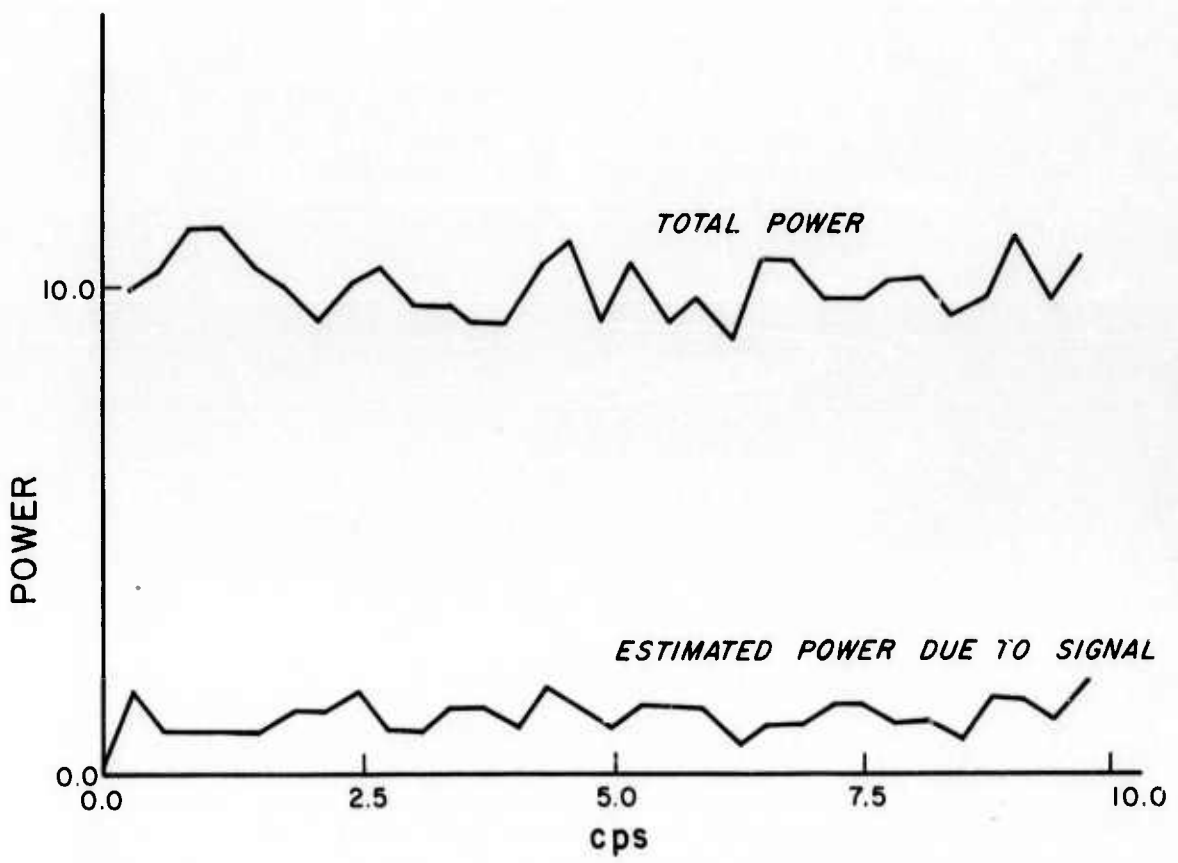

Figure 4. Analysis of power, Sig. Amp. = 0.0, Noise Power = 1.0, Number of Sensors = 10.

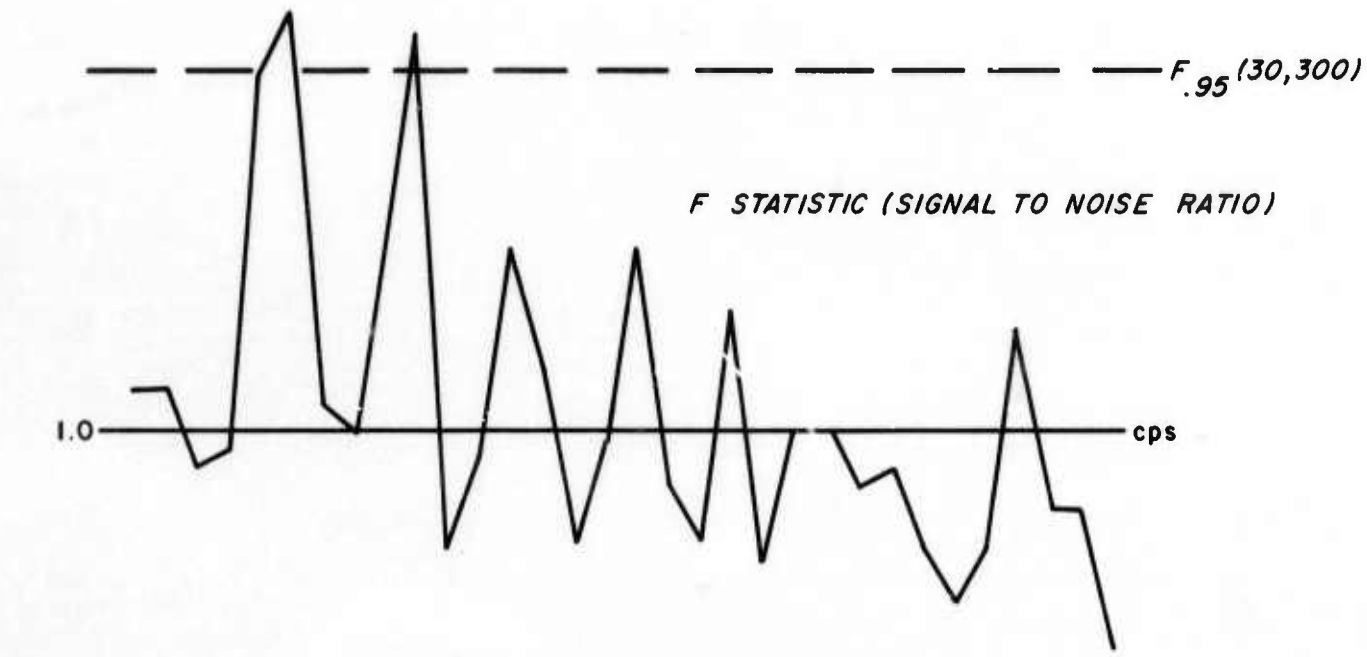

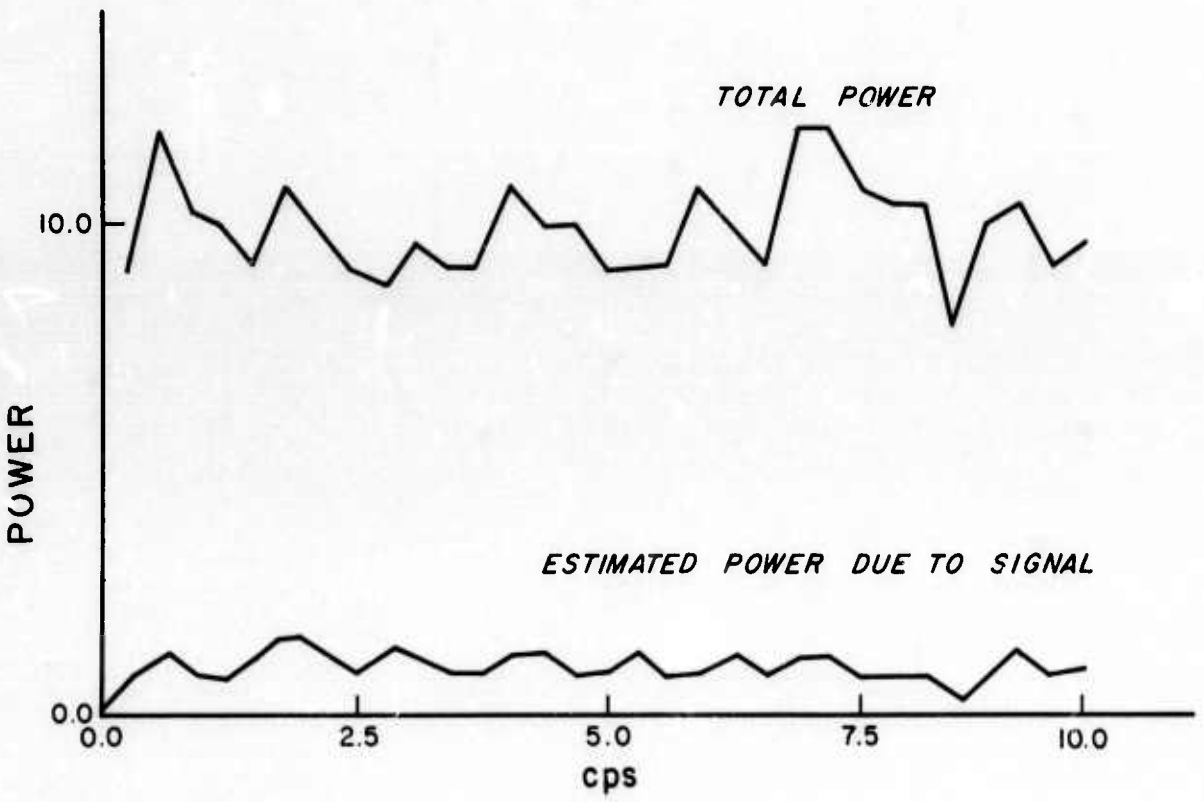

Figure 5. Analysis of power, Sig. Amp. = 0.5, Noise Power = 1.0, Number of Sensors = 10.

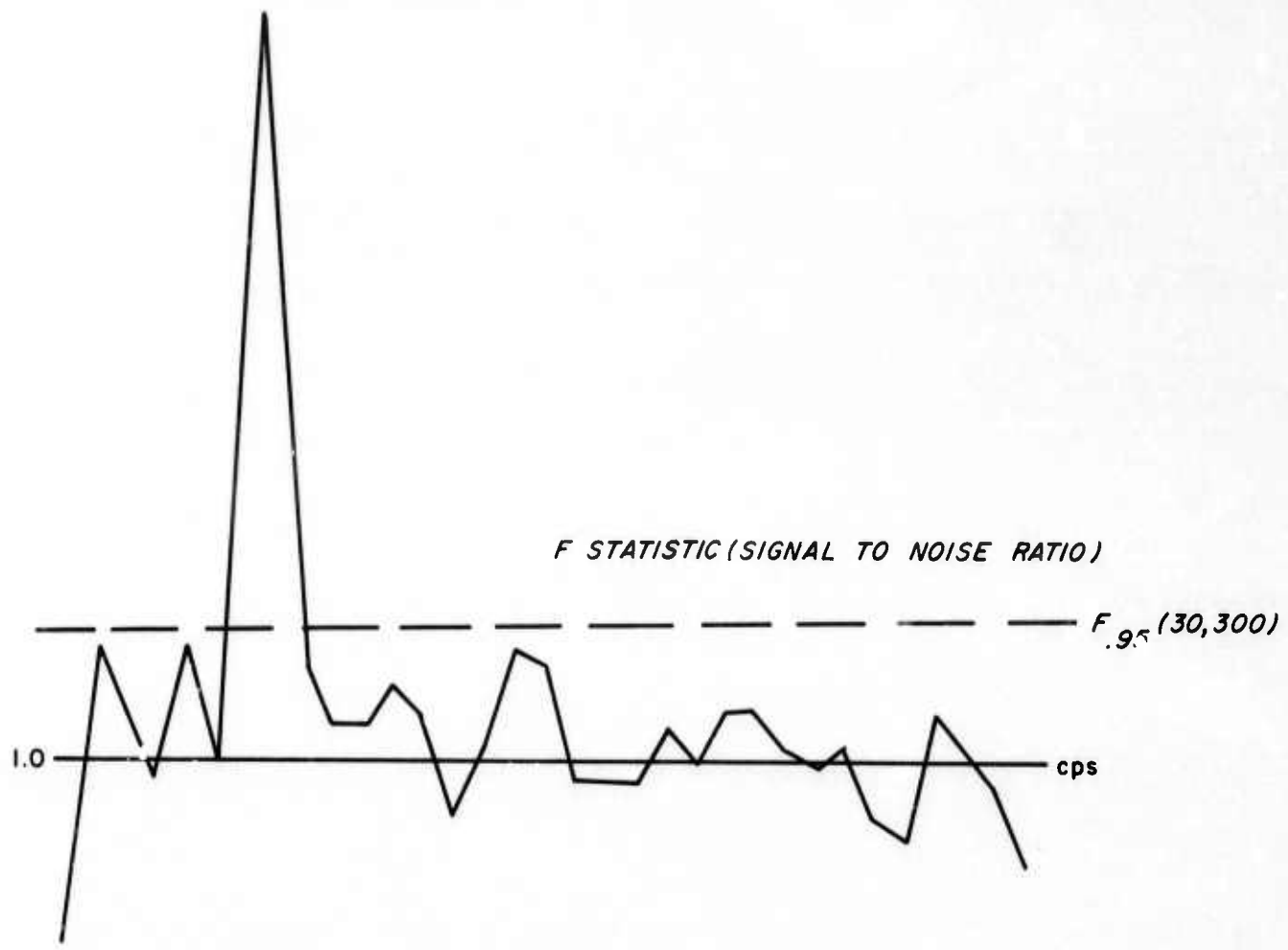

Figure 6. Analysis of power, Sig. Amp. = 1.0, Noise Power = 1.0, Number of Sensors = 10.

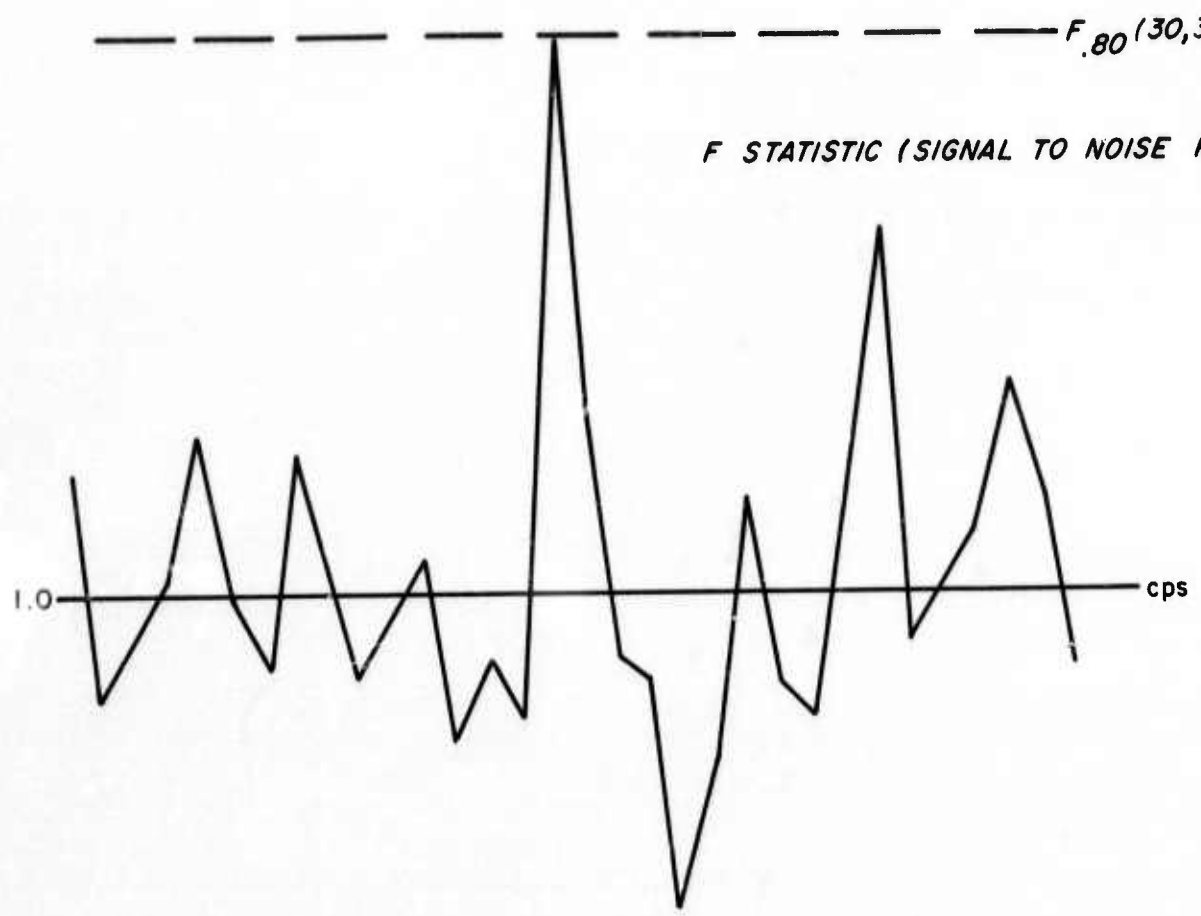

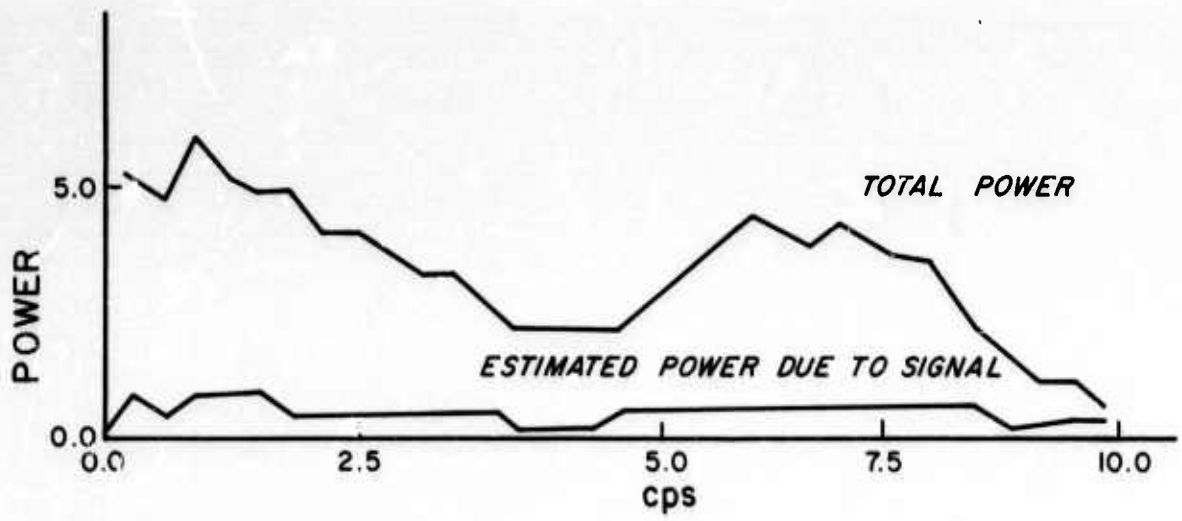

Figure 7. Analysis of power, Sig. Amp. = 0.0, Noise Power = 0.55, Number of Sensors = 10.

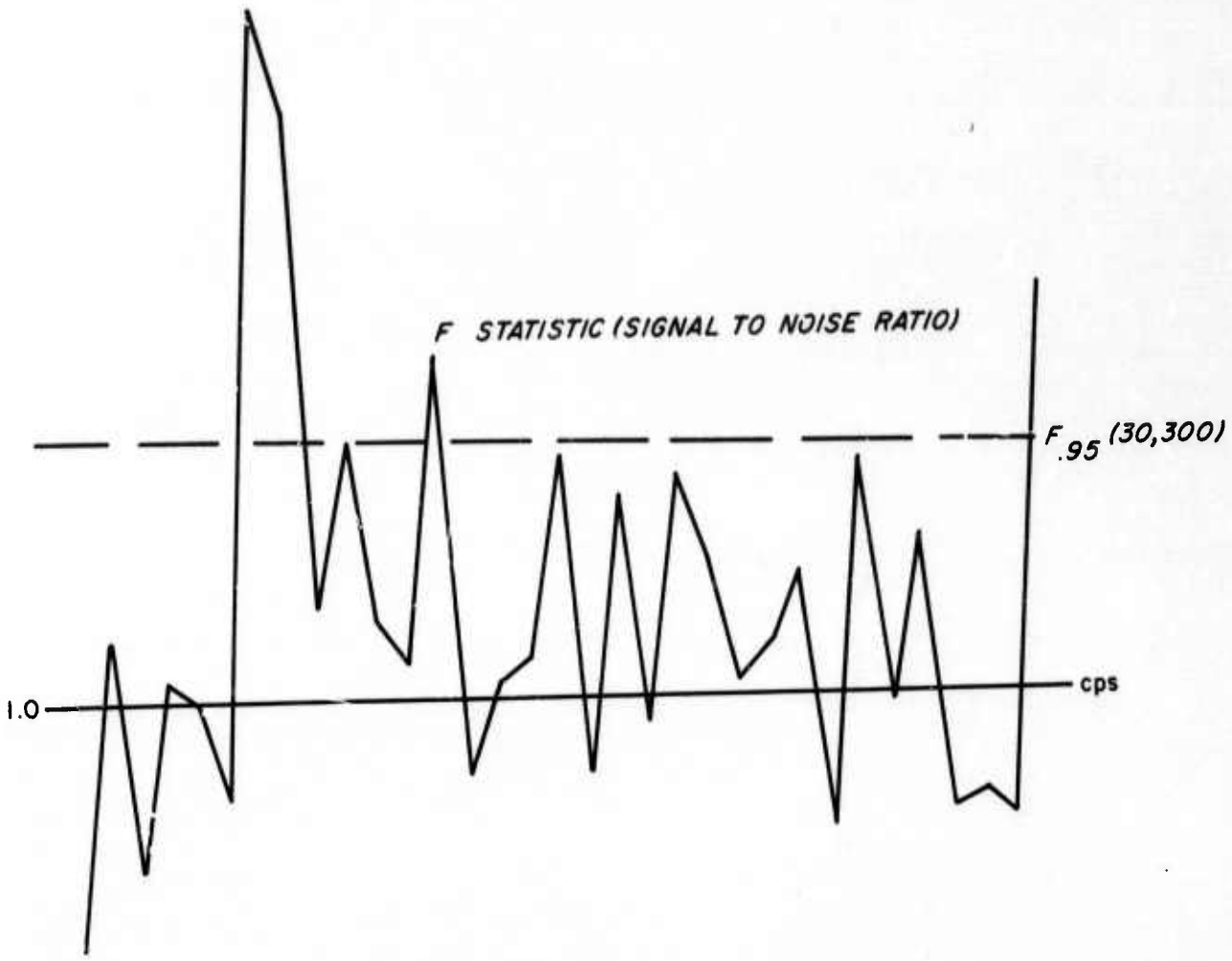

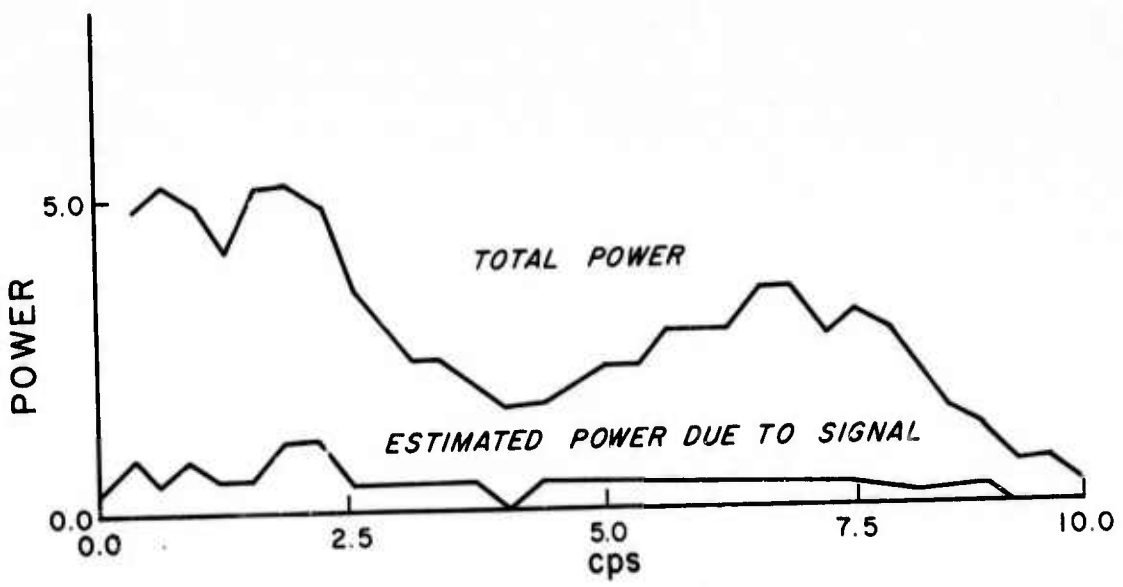

Figure 8. Analysis of power, Sig. Amp. = 0.5, Noise Power = 0.55, Number of Sensors = 10.

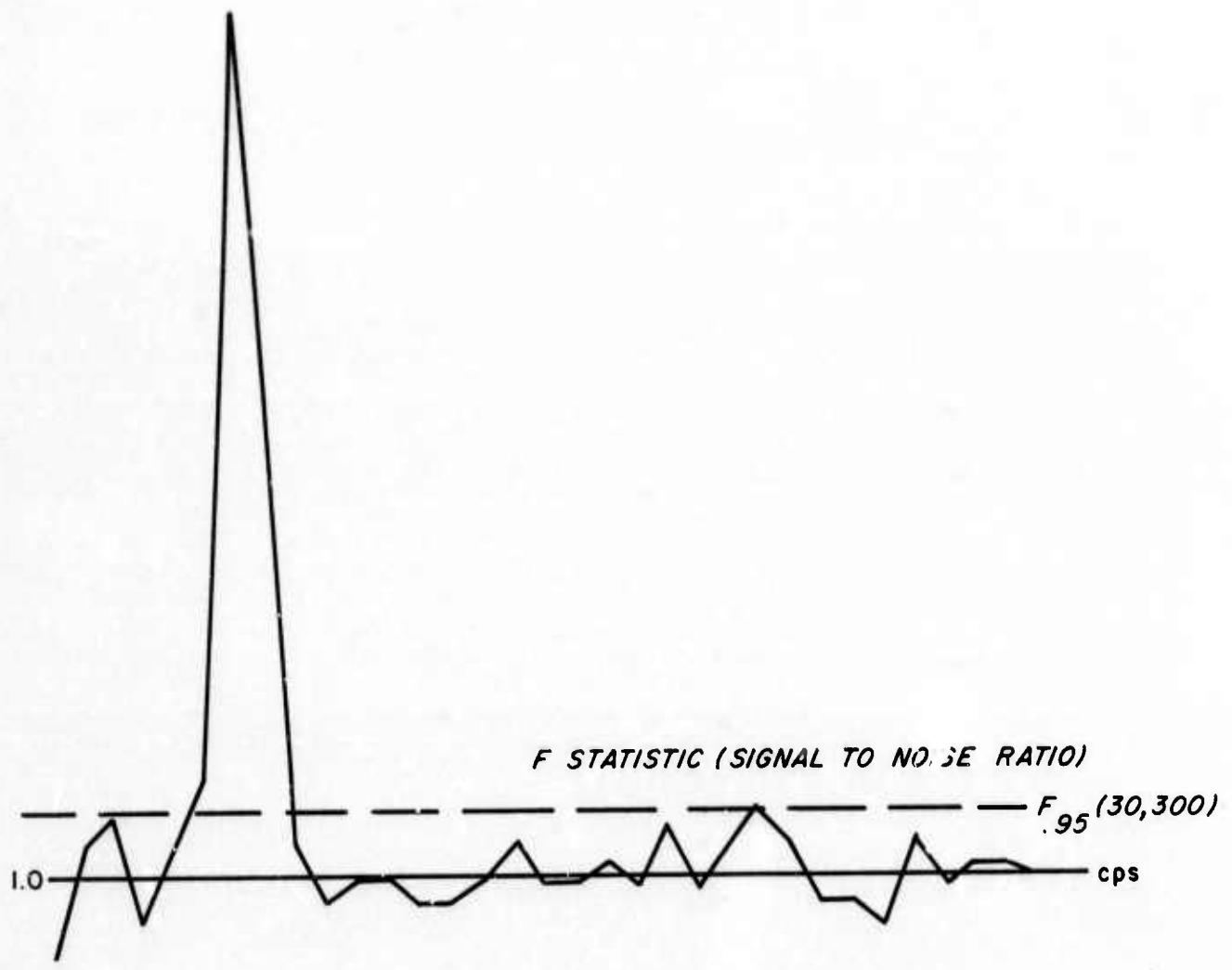

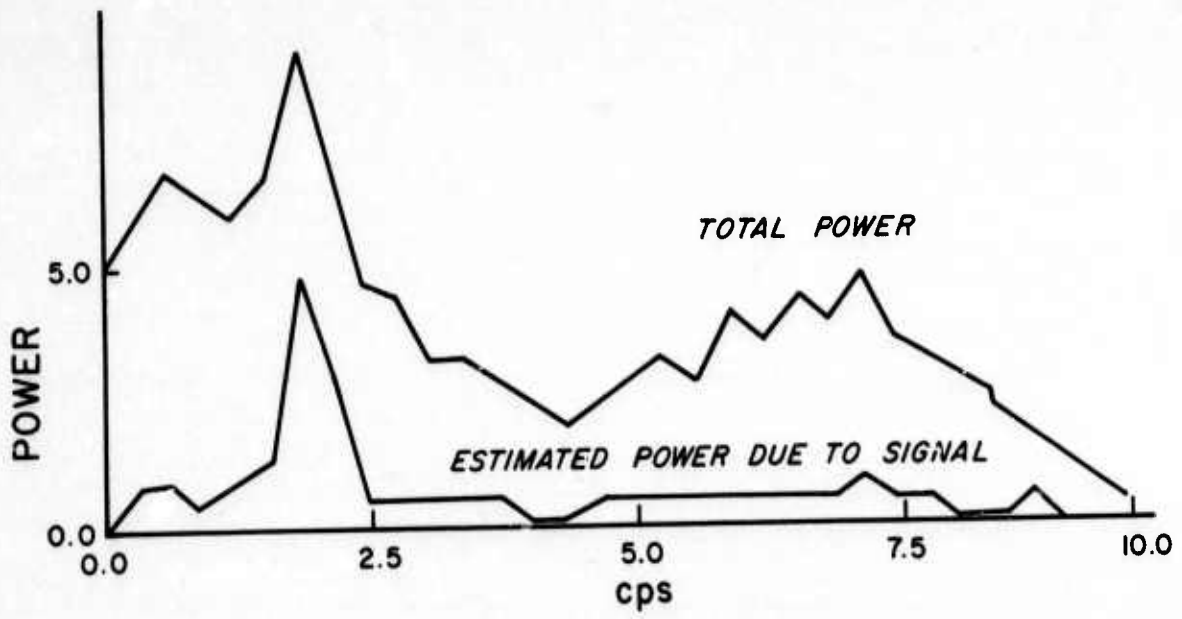

Figure 9. Analysis of power, Sig. Amp. = 1.0, Noise Power = 0.55, Number of Sensors = 10.

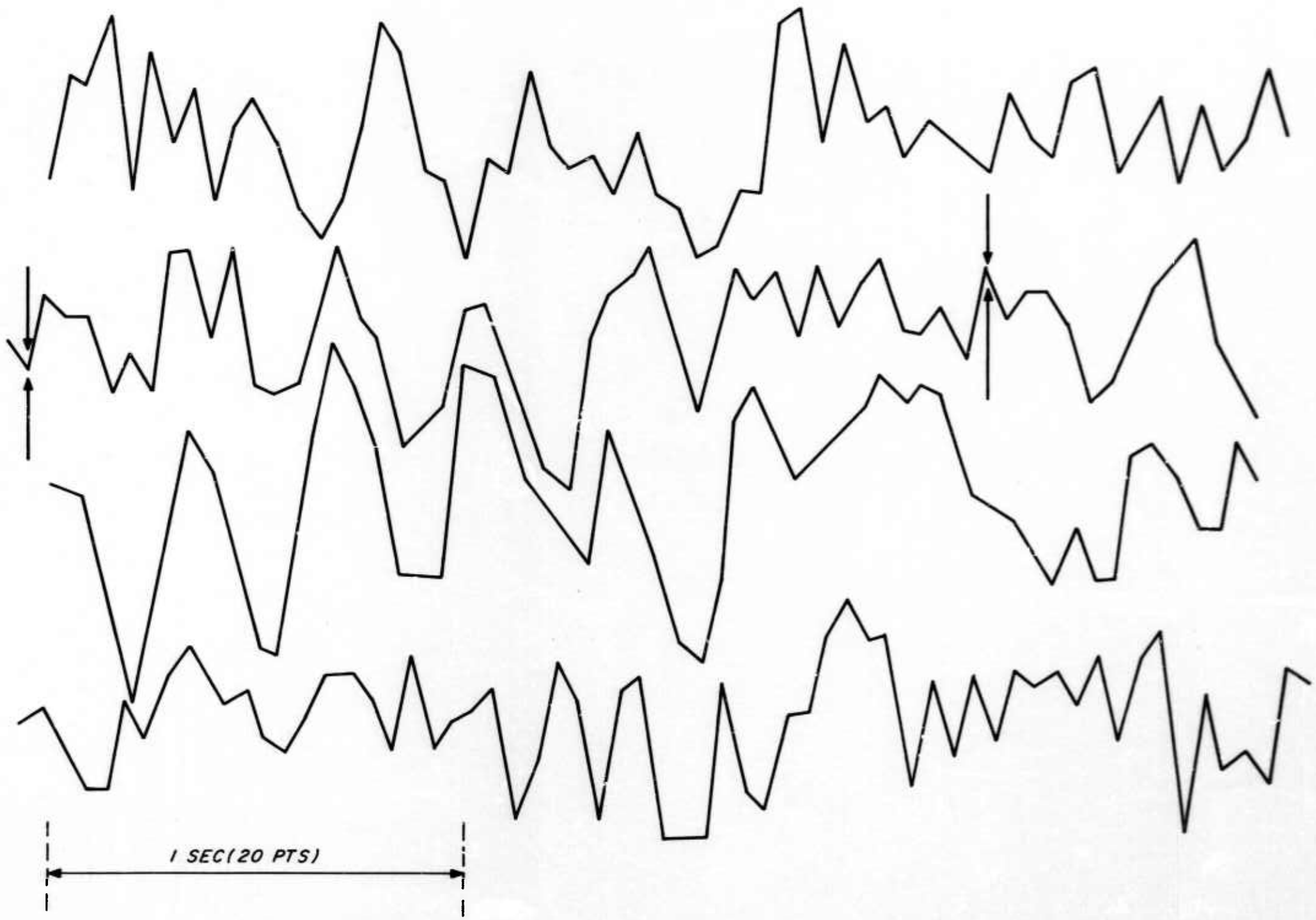

Figure 10. Observed time series
$Y_{10}(t) = n(t) + S(t-T_{10}) + S(t+T_{10}) + n_{10}(t)$

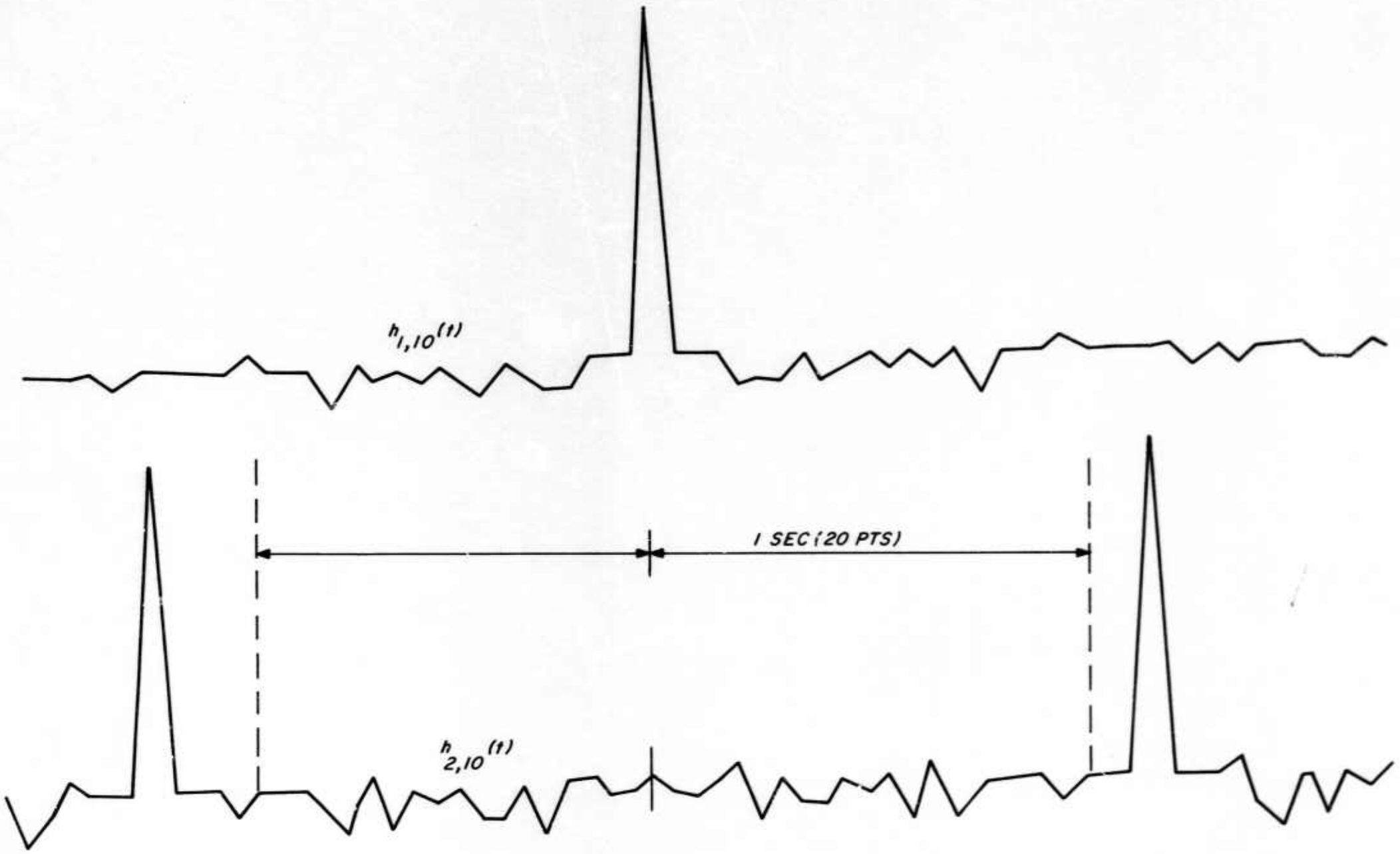

Figure 11. Filters for estimating n(t) and S(t).

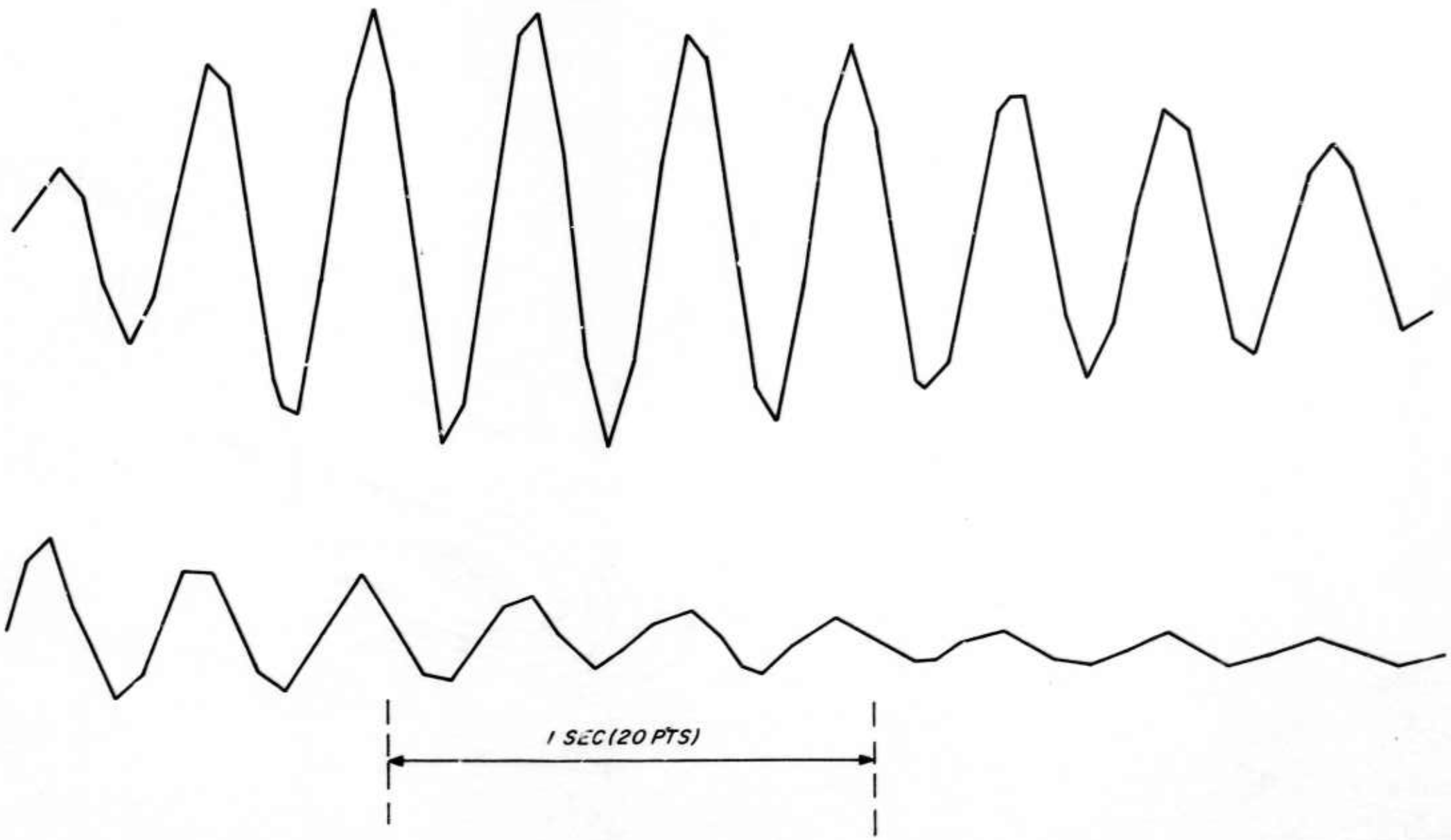

Figure 12. True signal S(t).

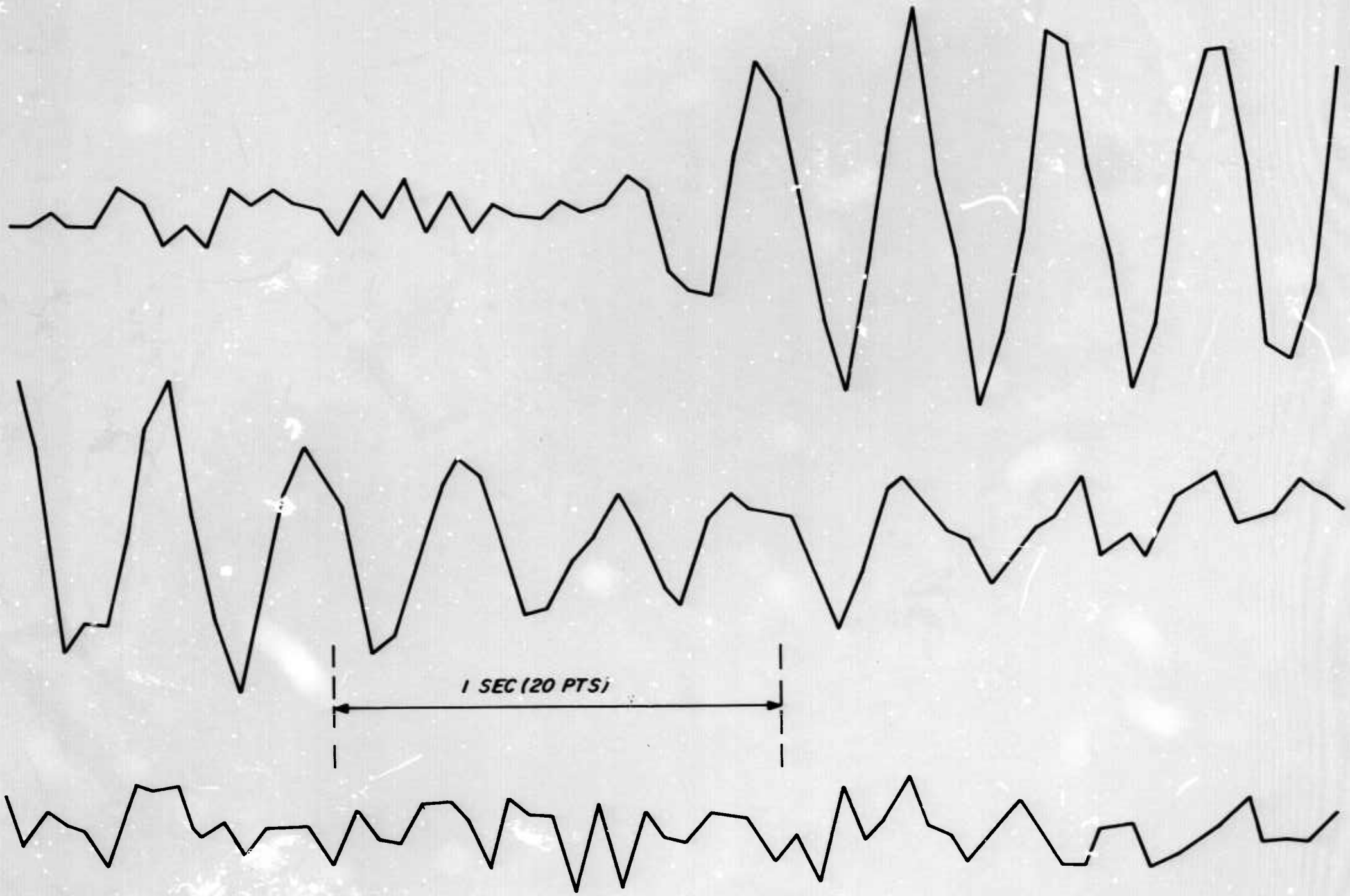

Figure 13. Estimated signal $\hat{S}(t)$.

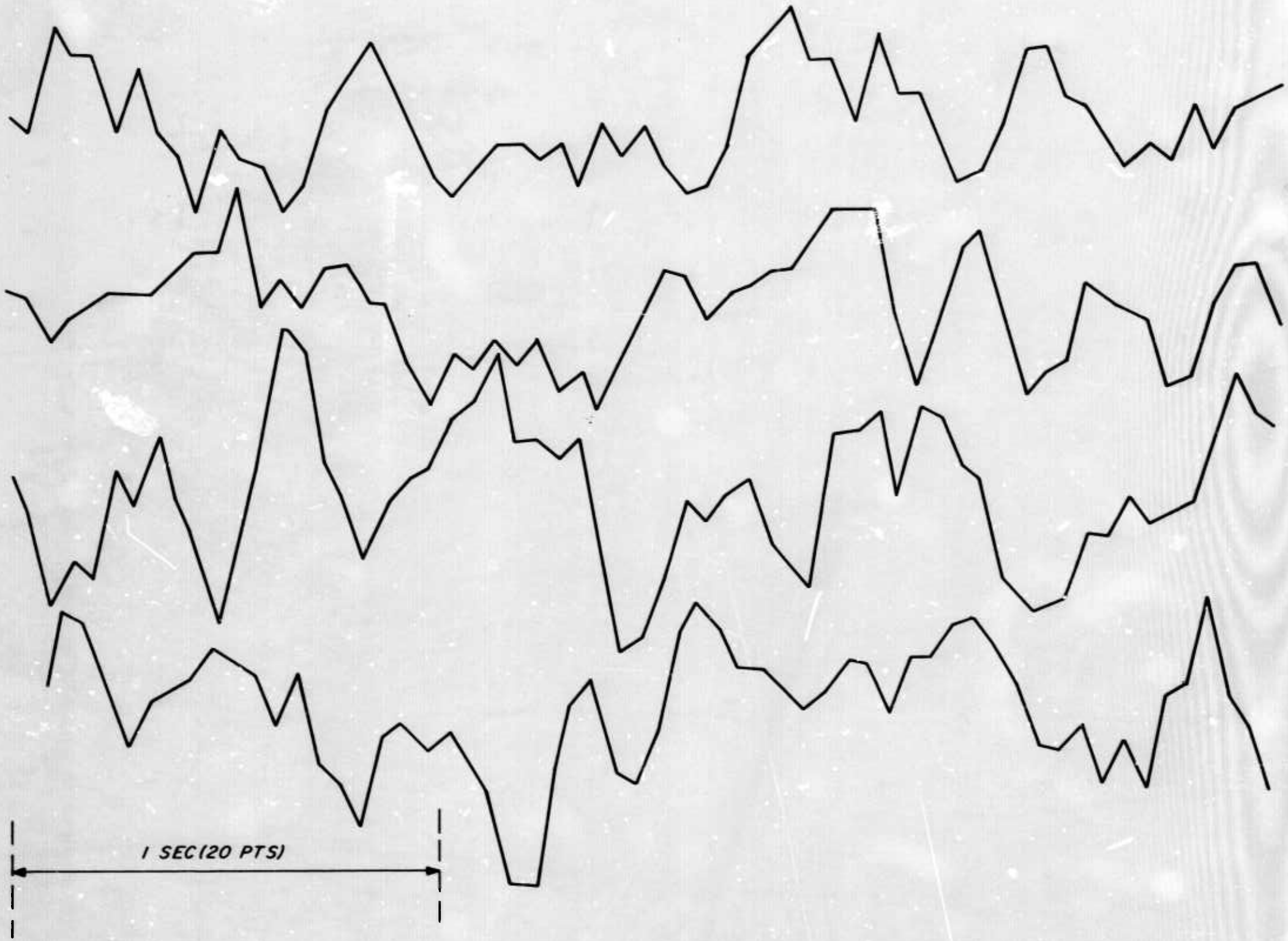

Figure 14. True noise n(t).

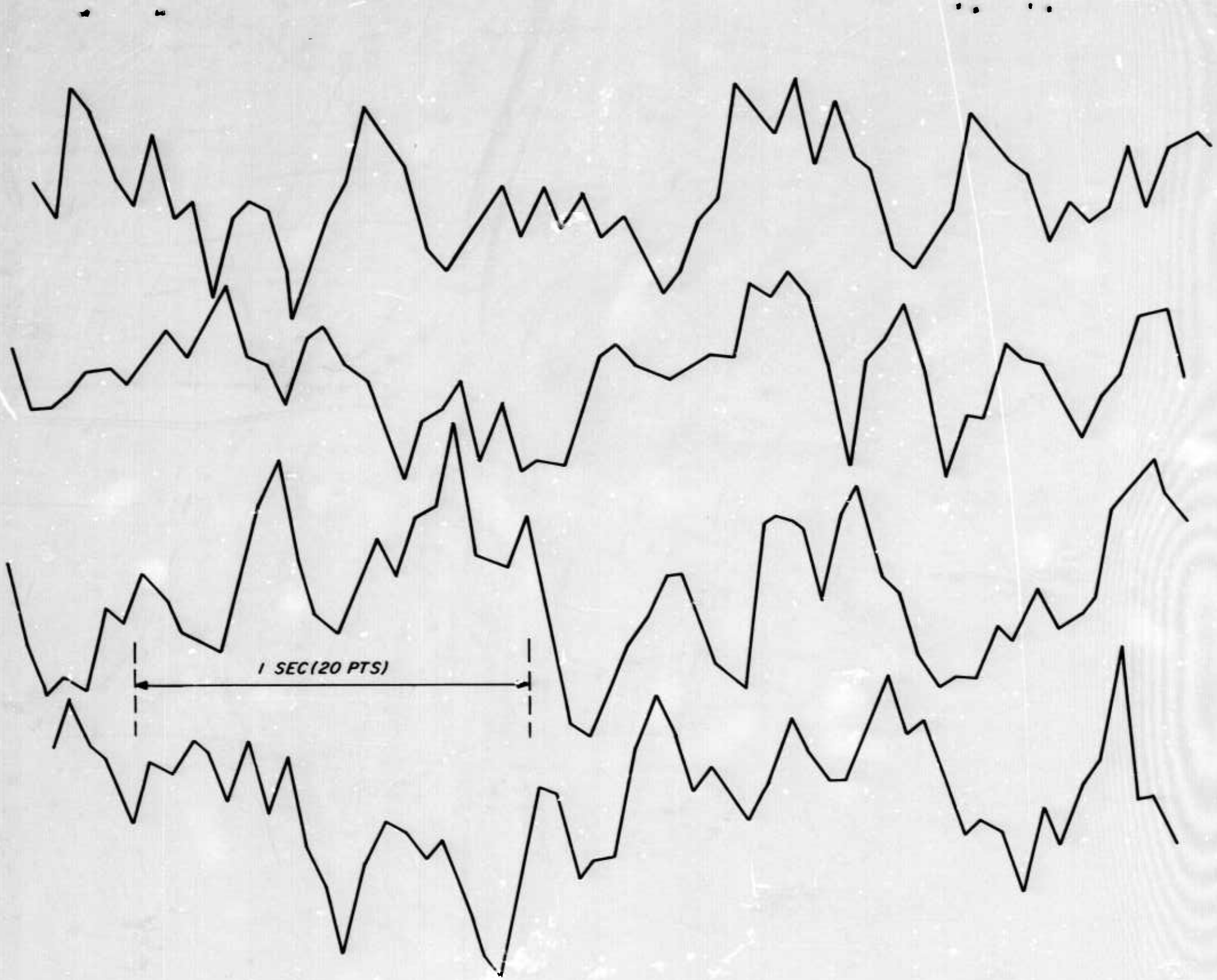

Figure 15. Estimated noise $\hat{n}(t)$.

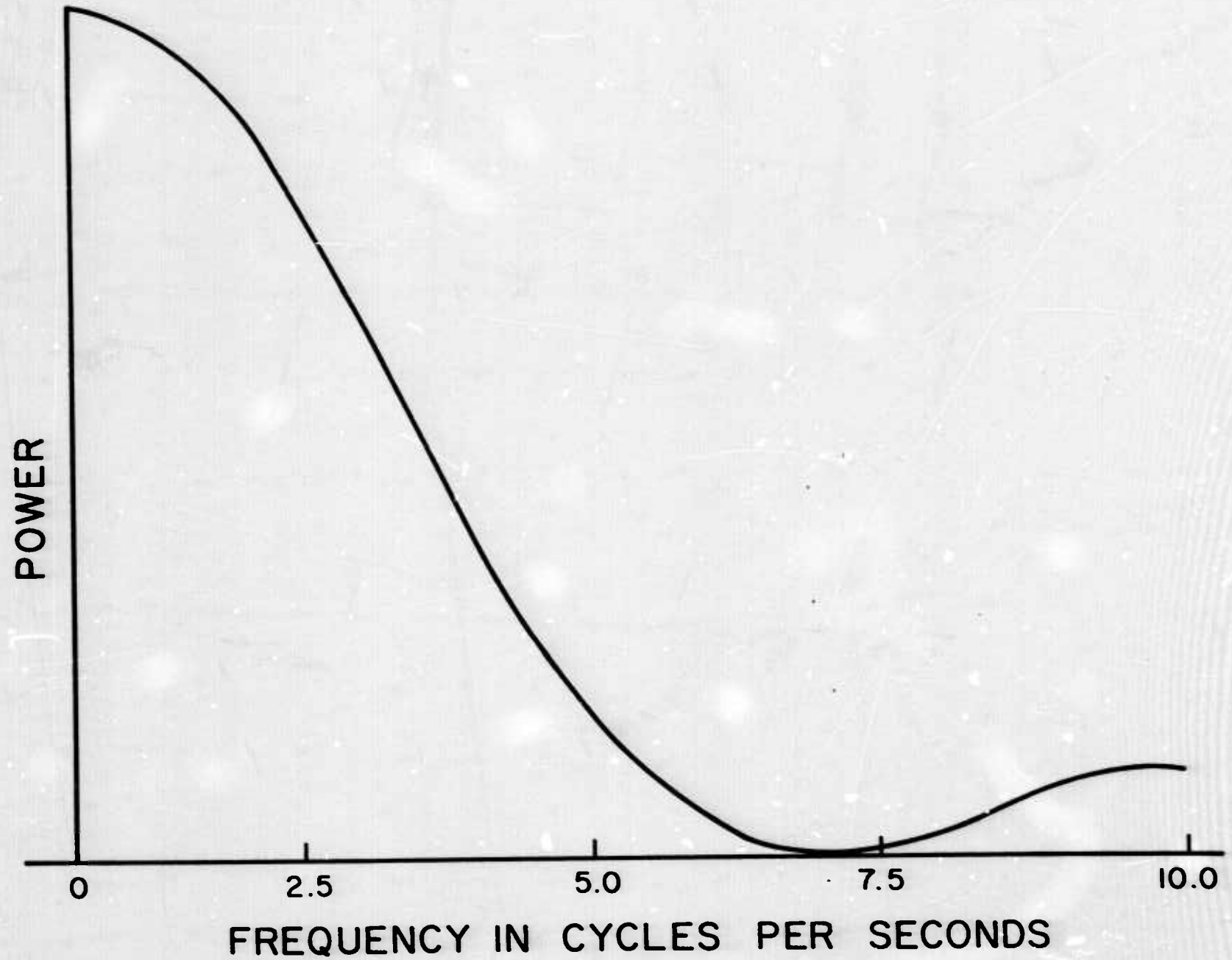

Figure 16. Theoretical power spectrum of coherent noise.

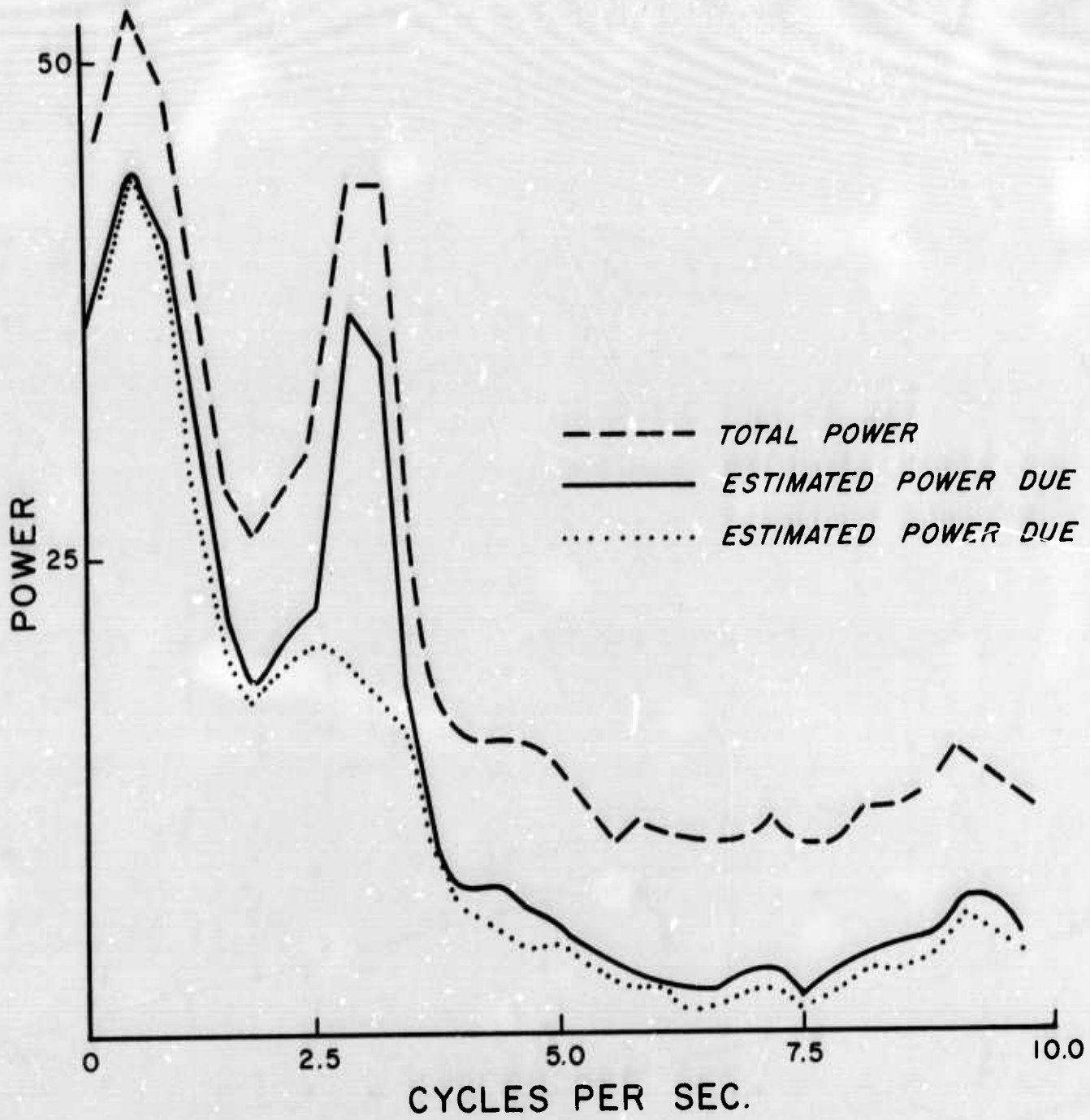

Figure 17. Analysis of power.

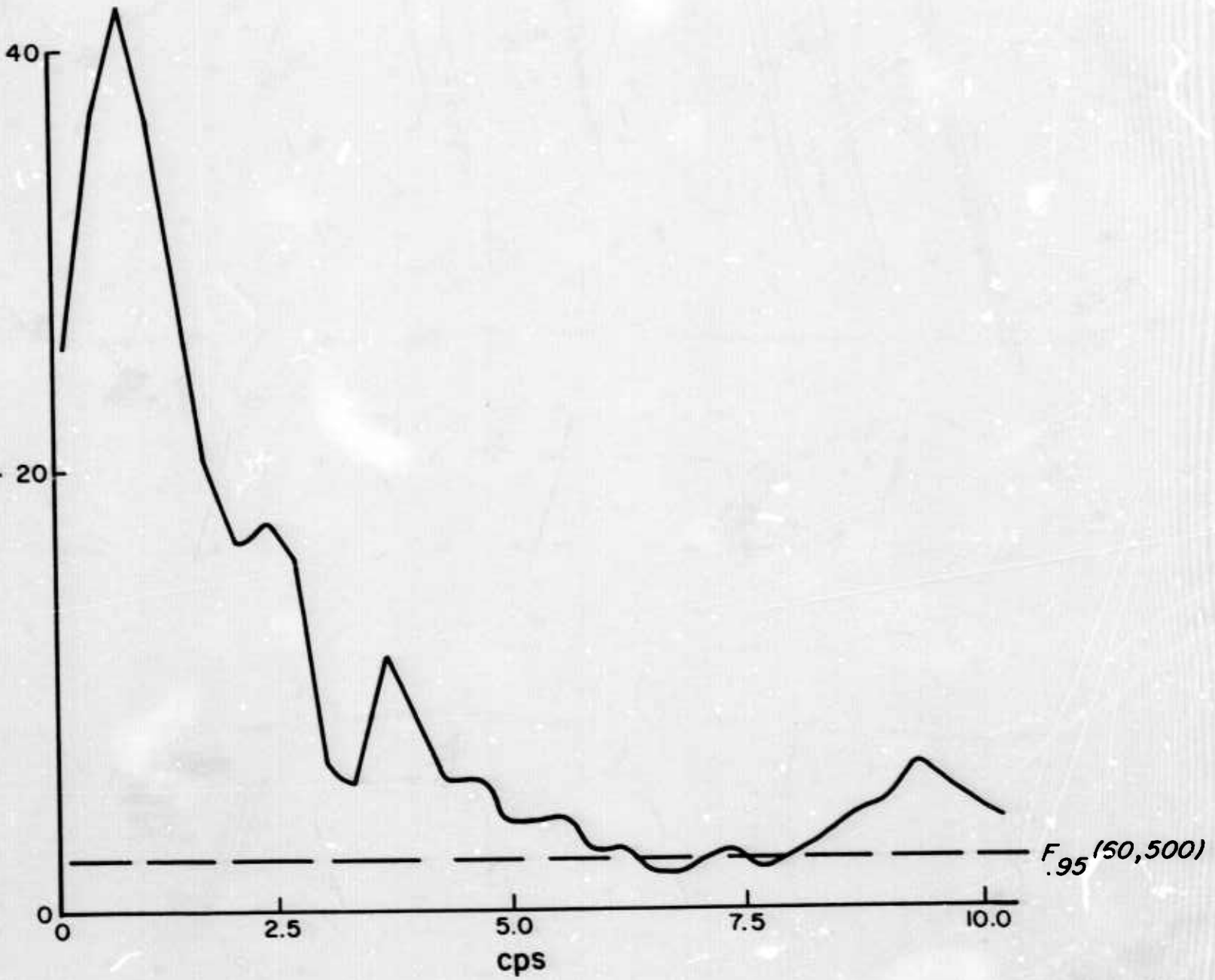

Figure 18. F statistic for testing hypothesis n(t) = 0.

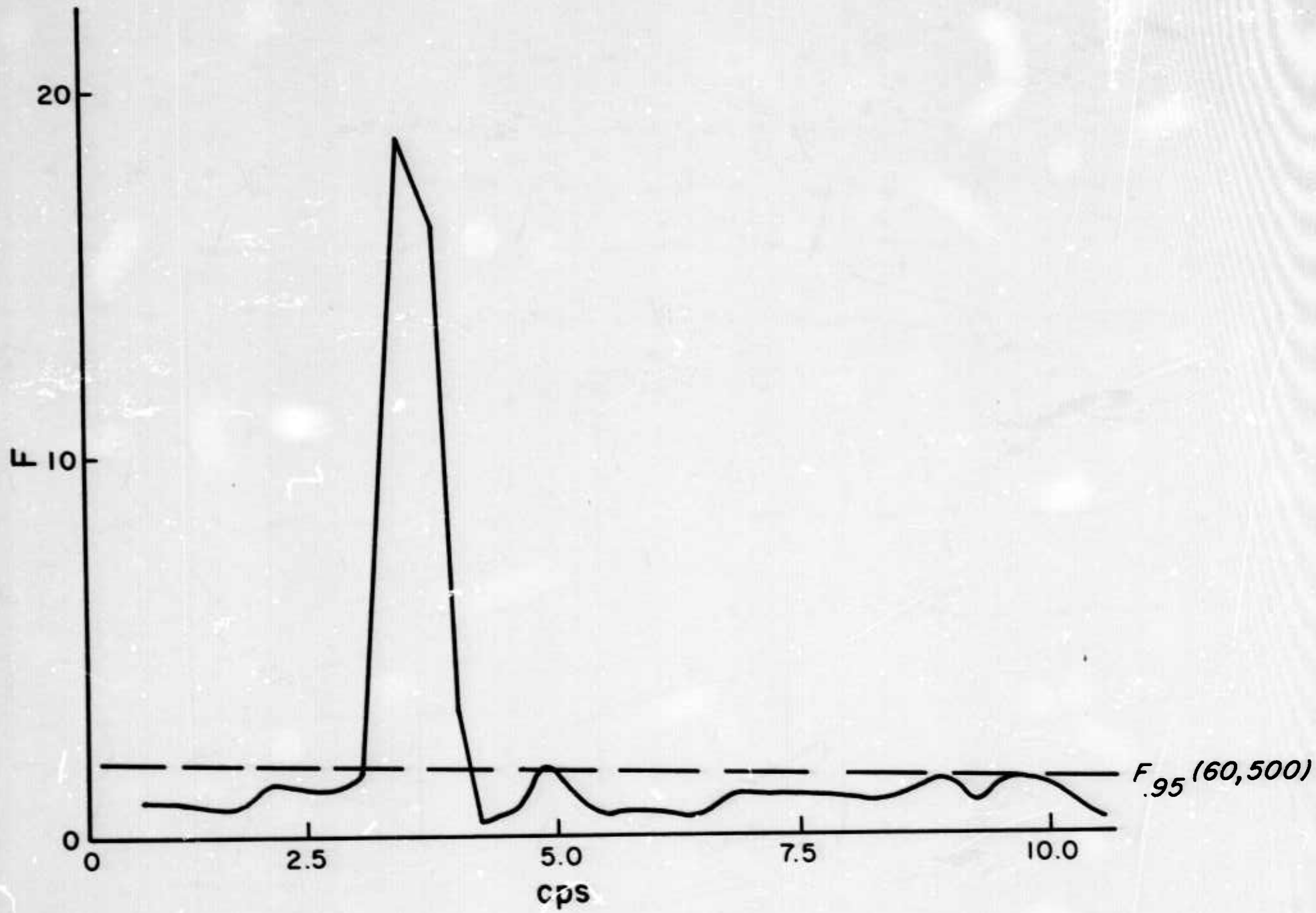

Figure 19. F statistic for testing hypothesis S(t) = 0 given n(t) ≠ 0.

Figure 20. Representative sample of LASA subarray contents Fiji Island, 26 September 1968.

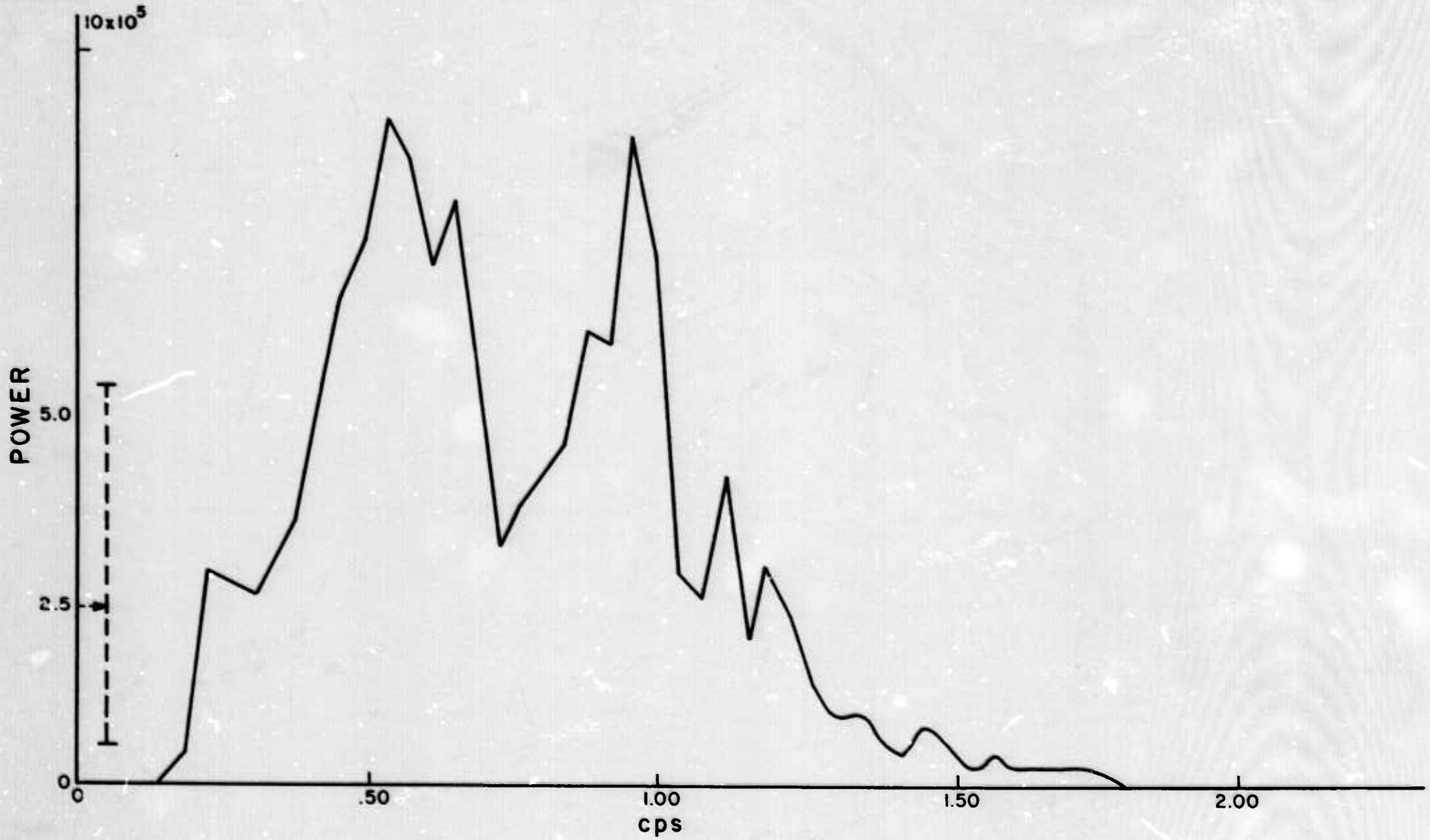

Figure 21. Estimated power due to signal (phased sum)
DF = 6, signal is present.

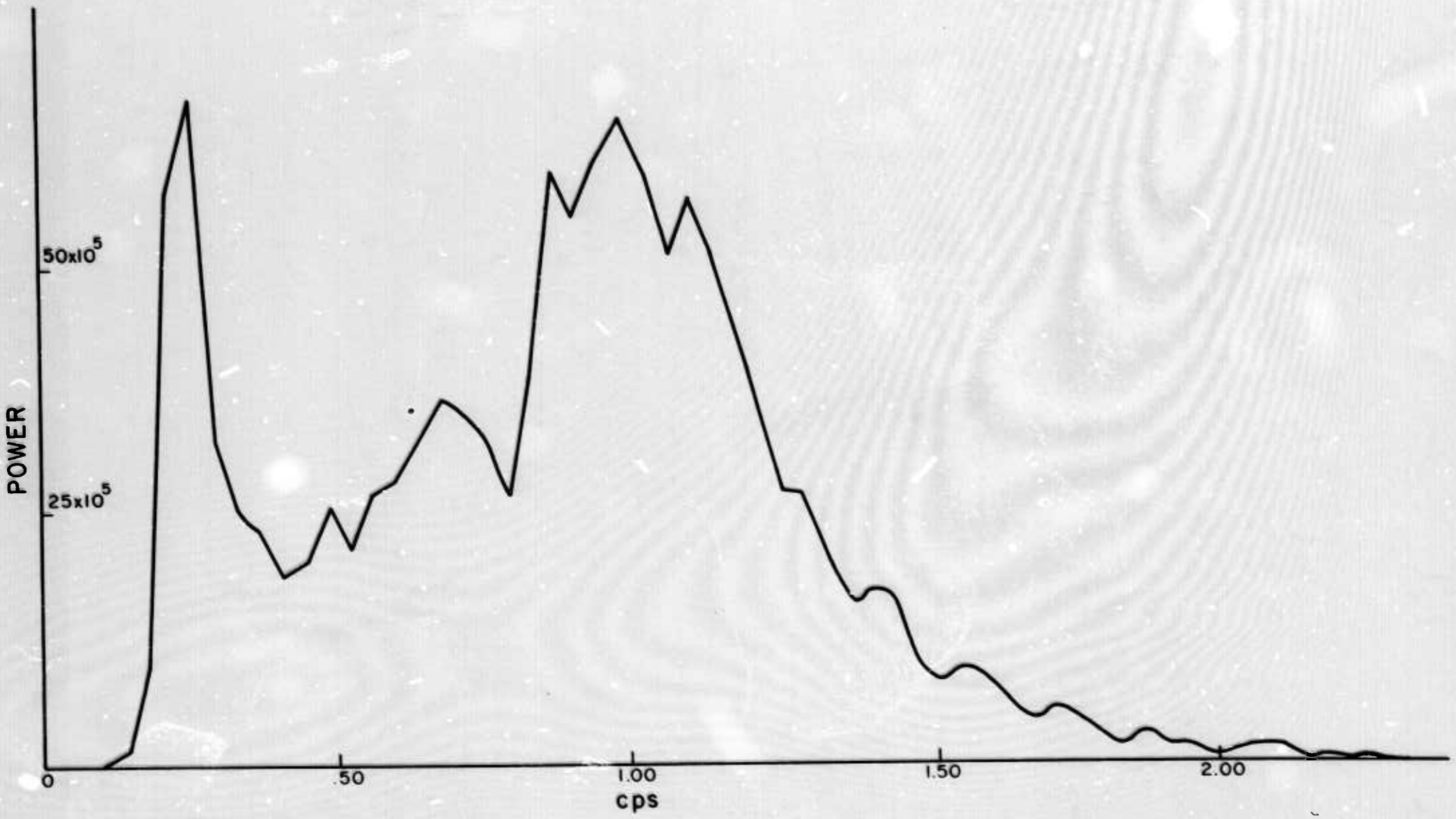

Figure 22. Estimated power due to noise DF = 120 signal is present.

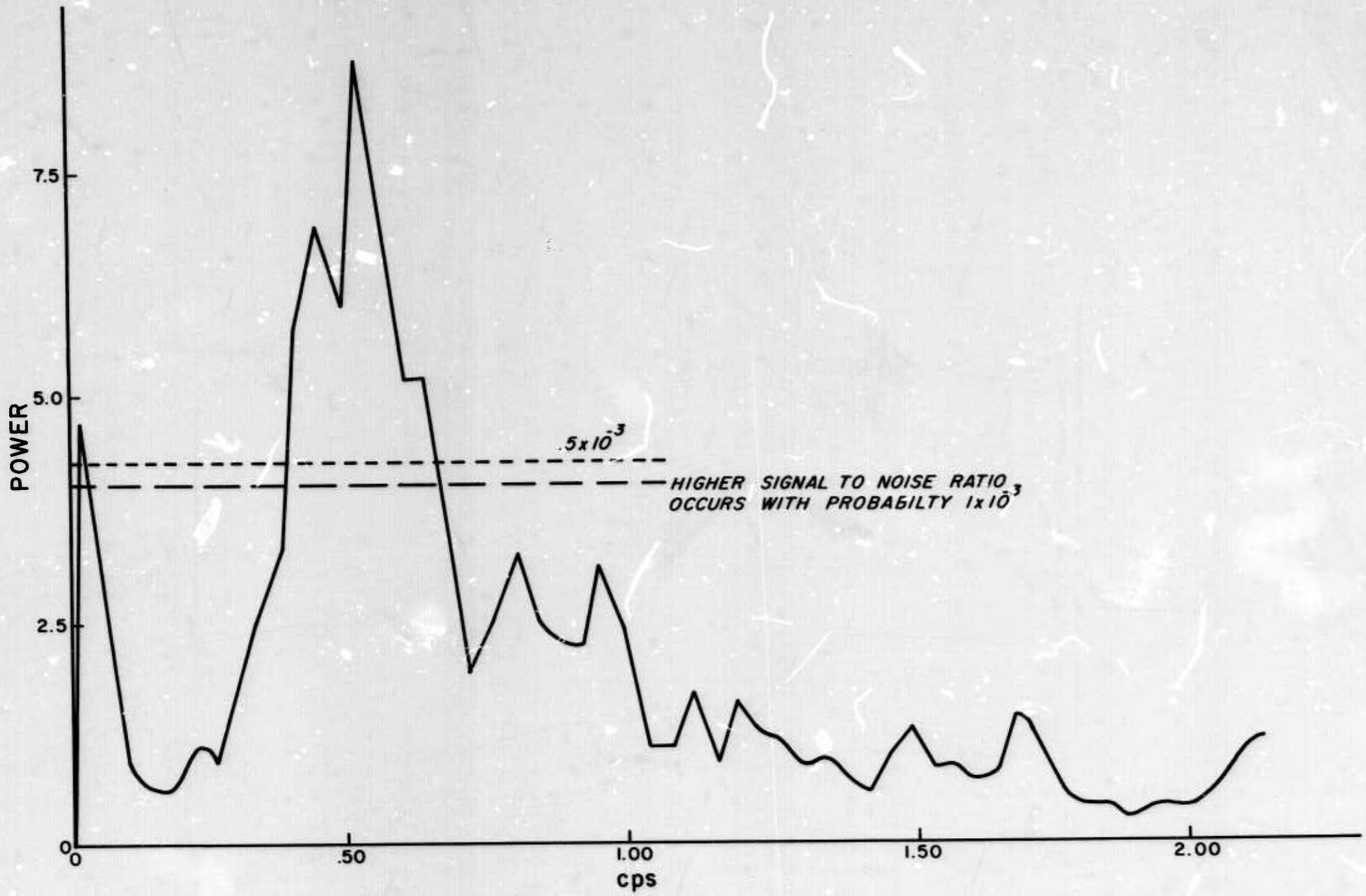

Figure 23. Signal to noise ratio F statistic with band 120 DF signal is present.

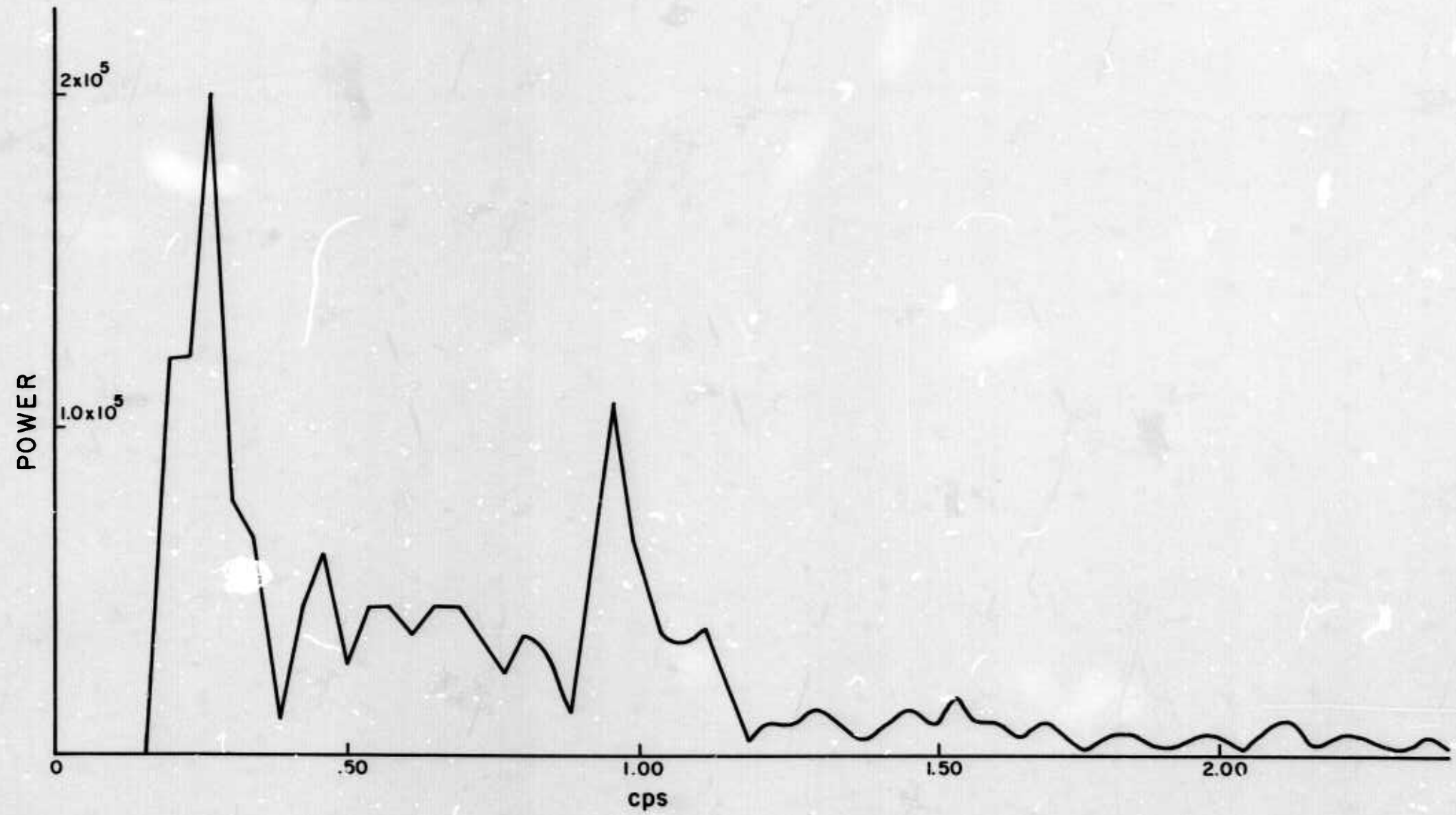

Figure 24. Estimated power due to signal (phased sum) DF = 6 signal is absent.

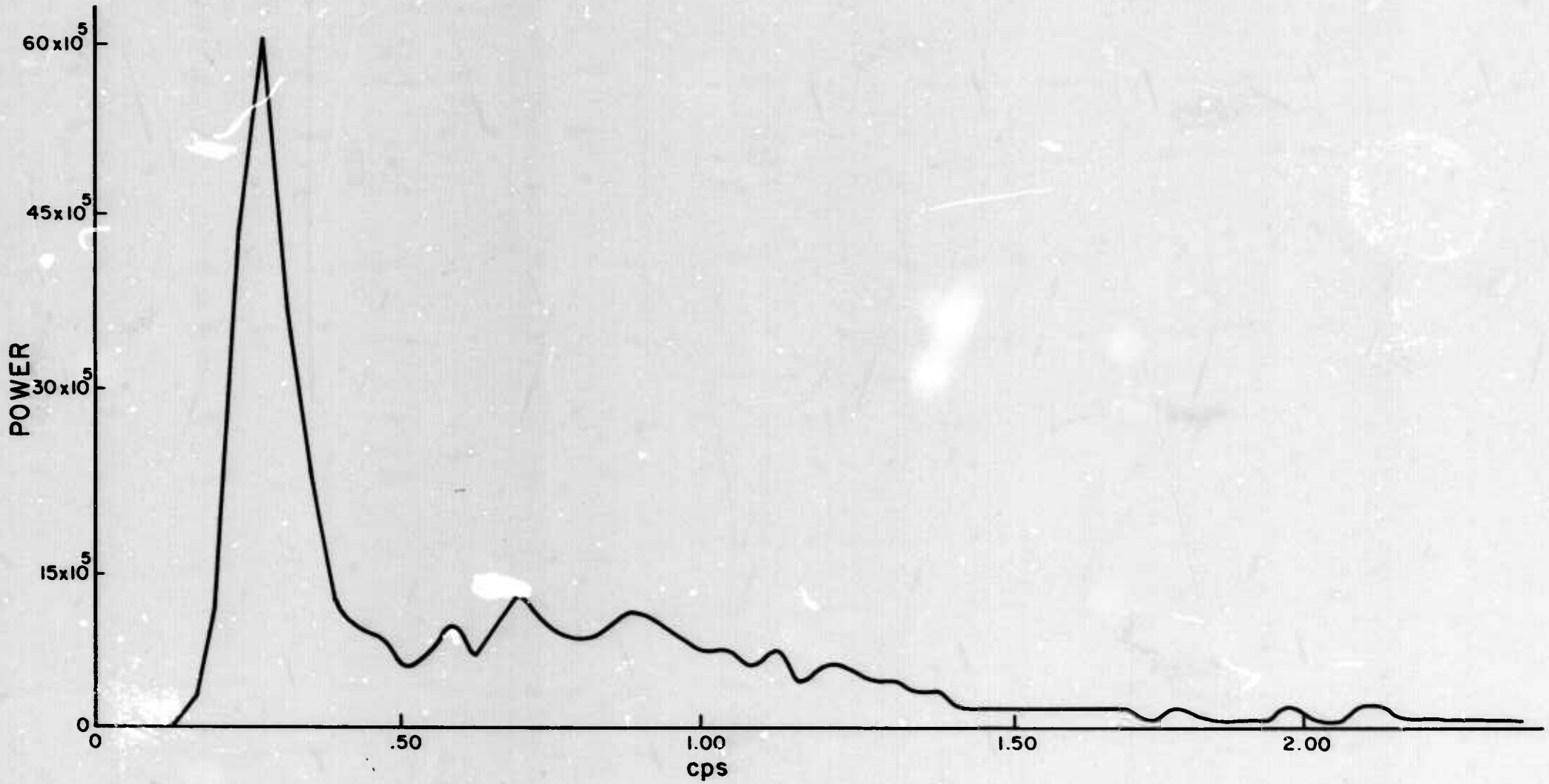

Figure 25. Estimated power due to noise DF = 120 signal is present.

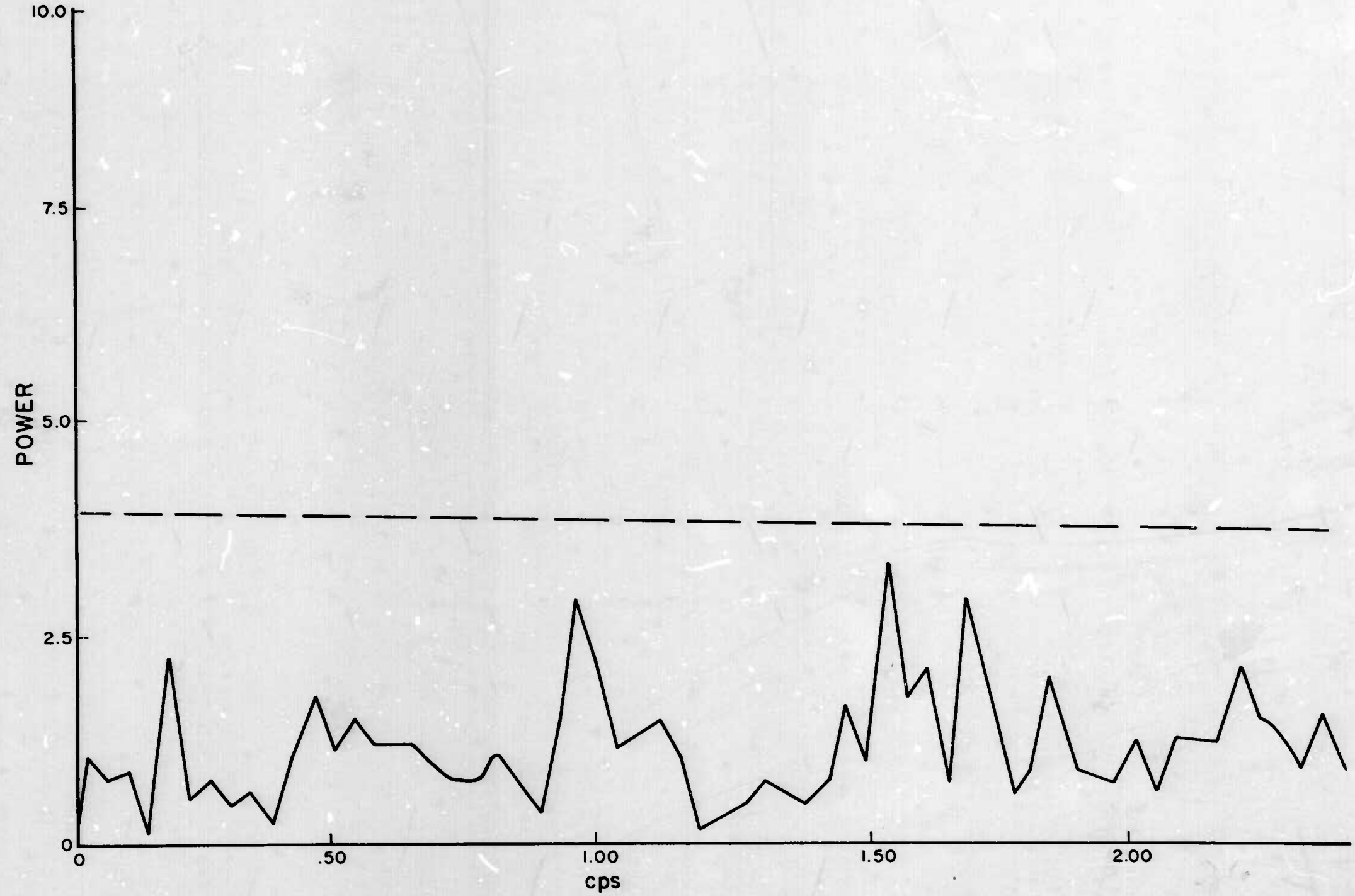

Figure 26. Signal to noise ratio F statistic with 6 and 120df signal is present.

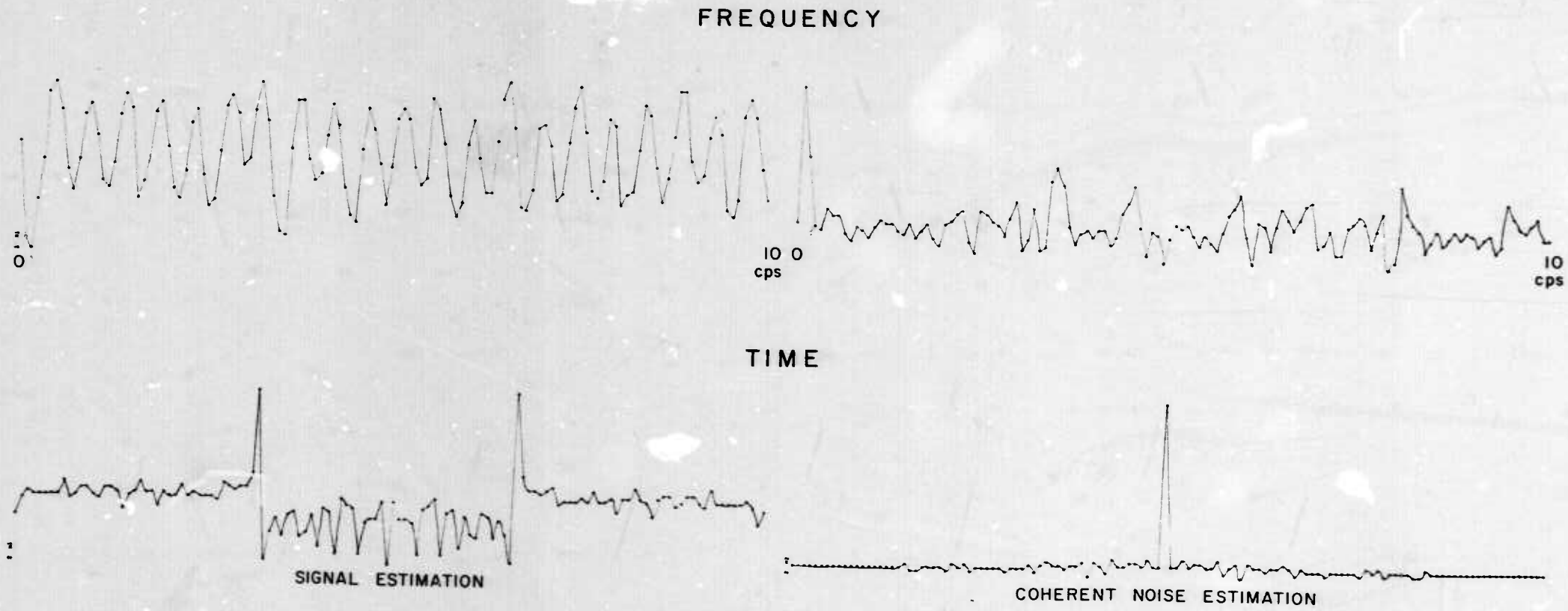

Figure : Full model maximum likelihood estimation filters for vertical array (128 pts).

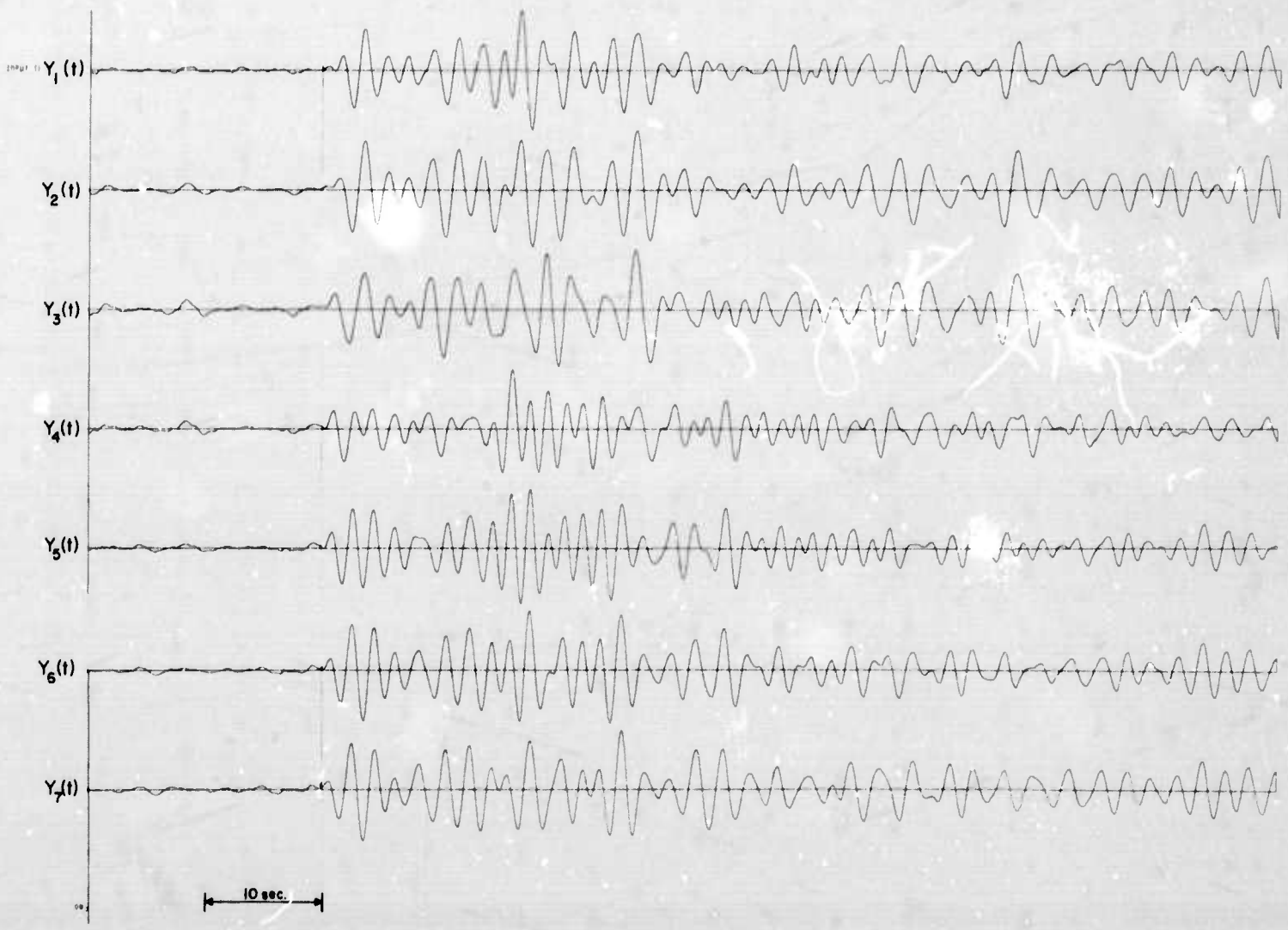

Figure 28. Input seismic traces containing signal from vertical array recording event from Fiji Islands (seismogram 14007).

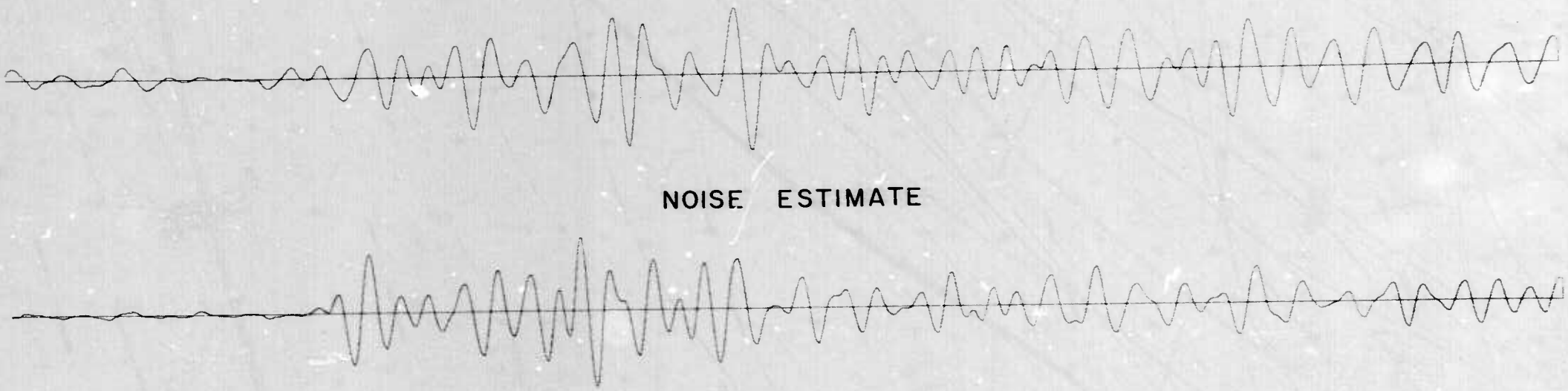

Figure 29. Signal and coherent noise estimates for Fiji Island event (full model).

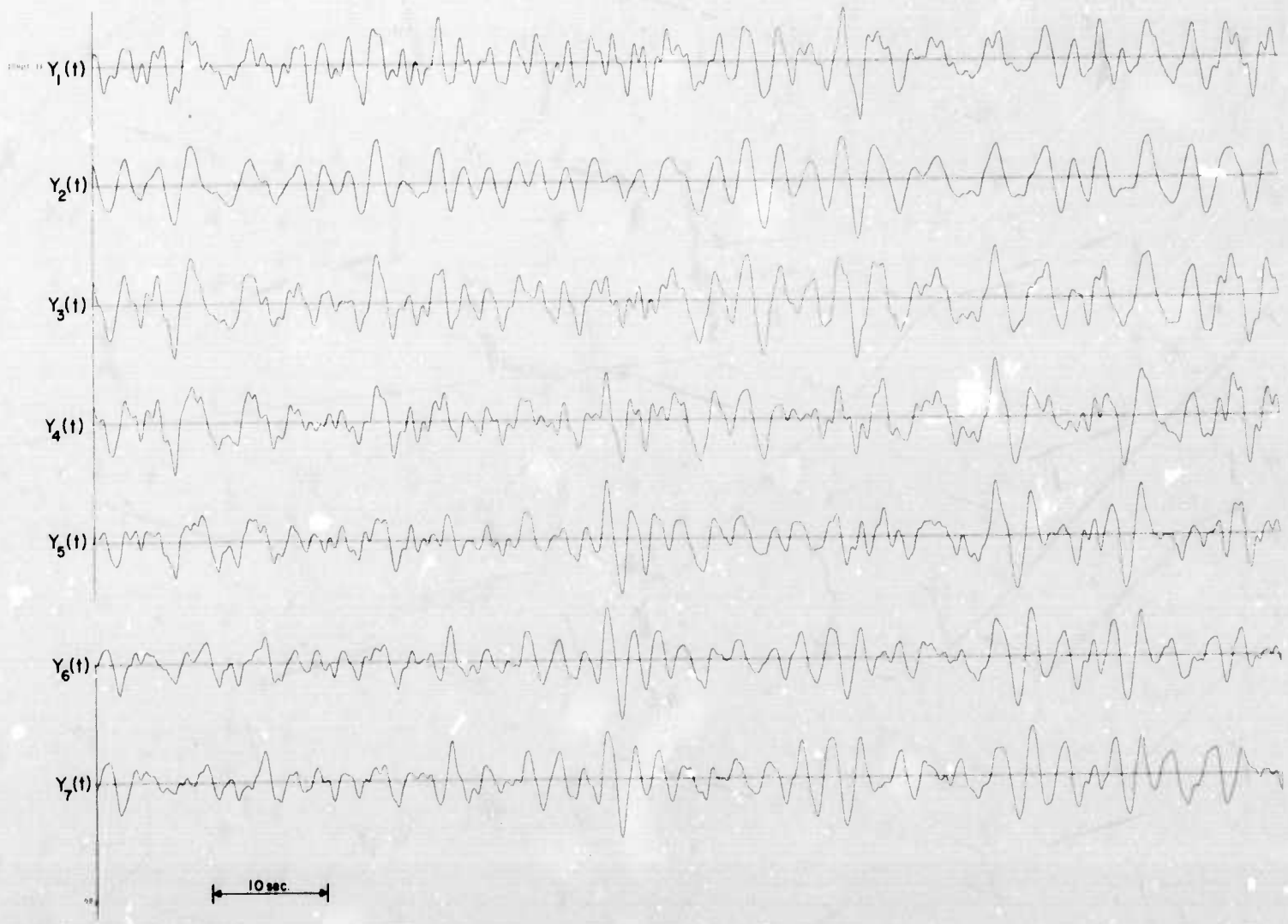

Figure 30. Input seismic traces containing noise from vertical array recording event from Fiji Islands (seismogram 14007).

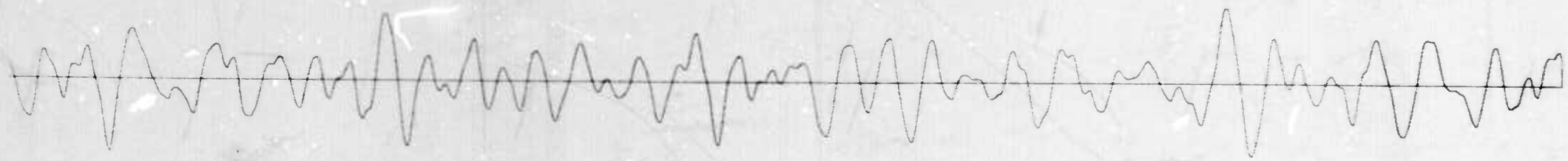

NOISE ESTIMATE

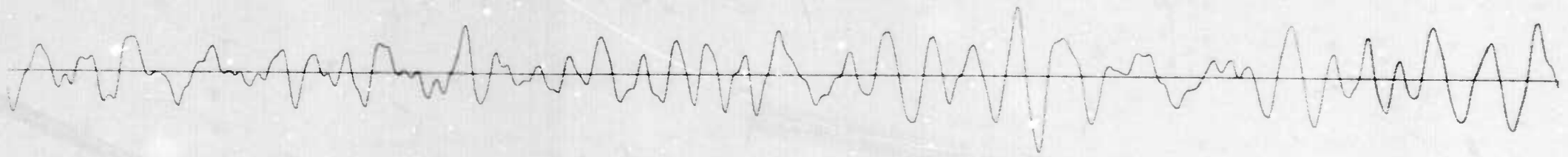

SIGNAL ESTIMATE

10 sec.

Figure 31. Signal and coherent noise estimates for Fiji Island event with data containing only noise.

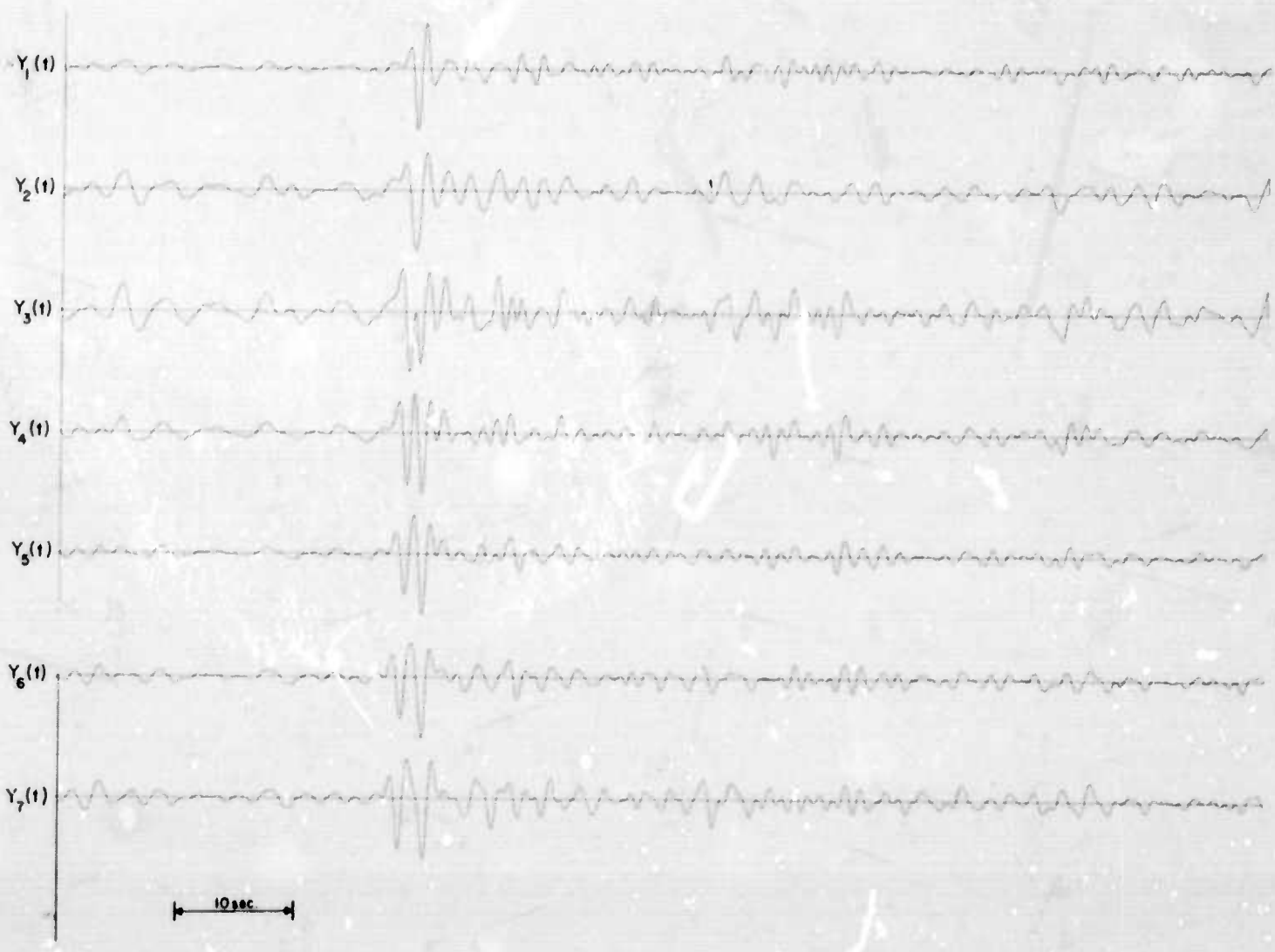

Figure 32. Input seismic traces containing signal from vertical array recording an event from Colombia (seismogram 14012).

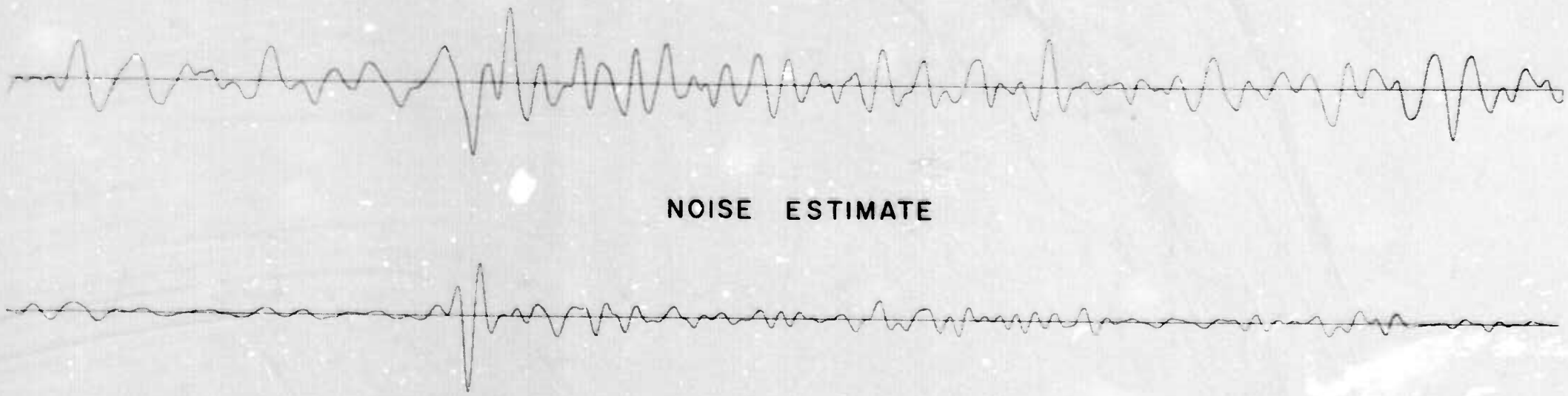

Figure 33. Signal and coherent noise estimates for Colombian event (full model).

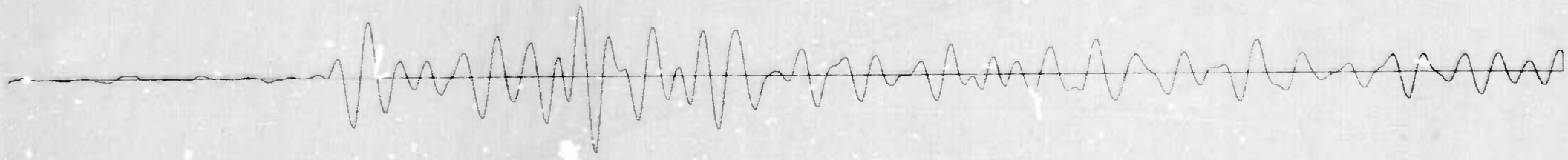

Figure 34. Signal estimate for Fiji Island event (reduced model).

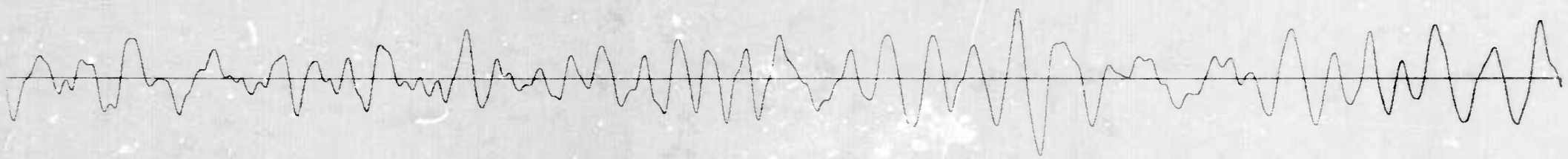

Figure 35. Signal estimate for Fiji Island event with data containing only noise.

SIGNAL ESTIMATE

10sec.

Figure 36. Signal estimates for Colombian event (reduced model).

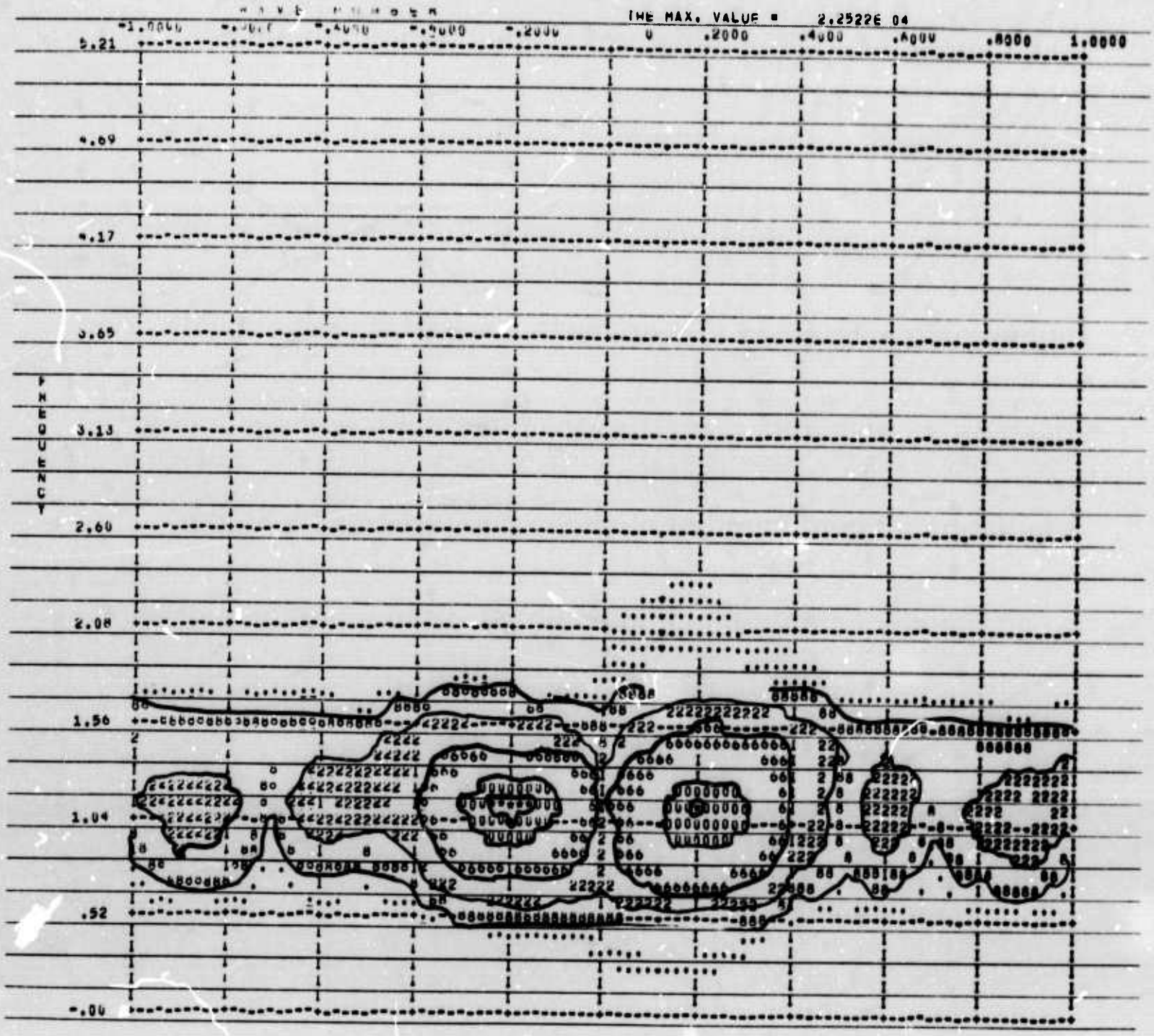

Figure 37. Frequency wave number analysis with signal and noise present for Fiji Island event.

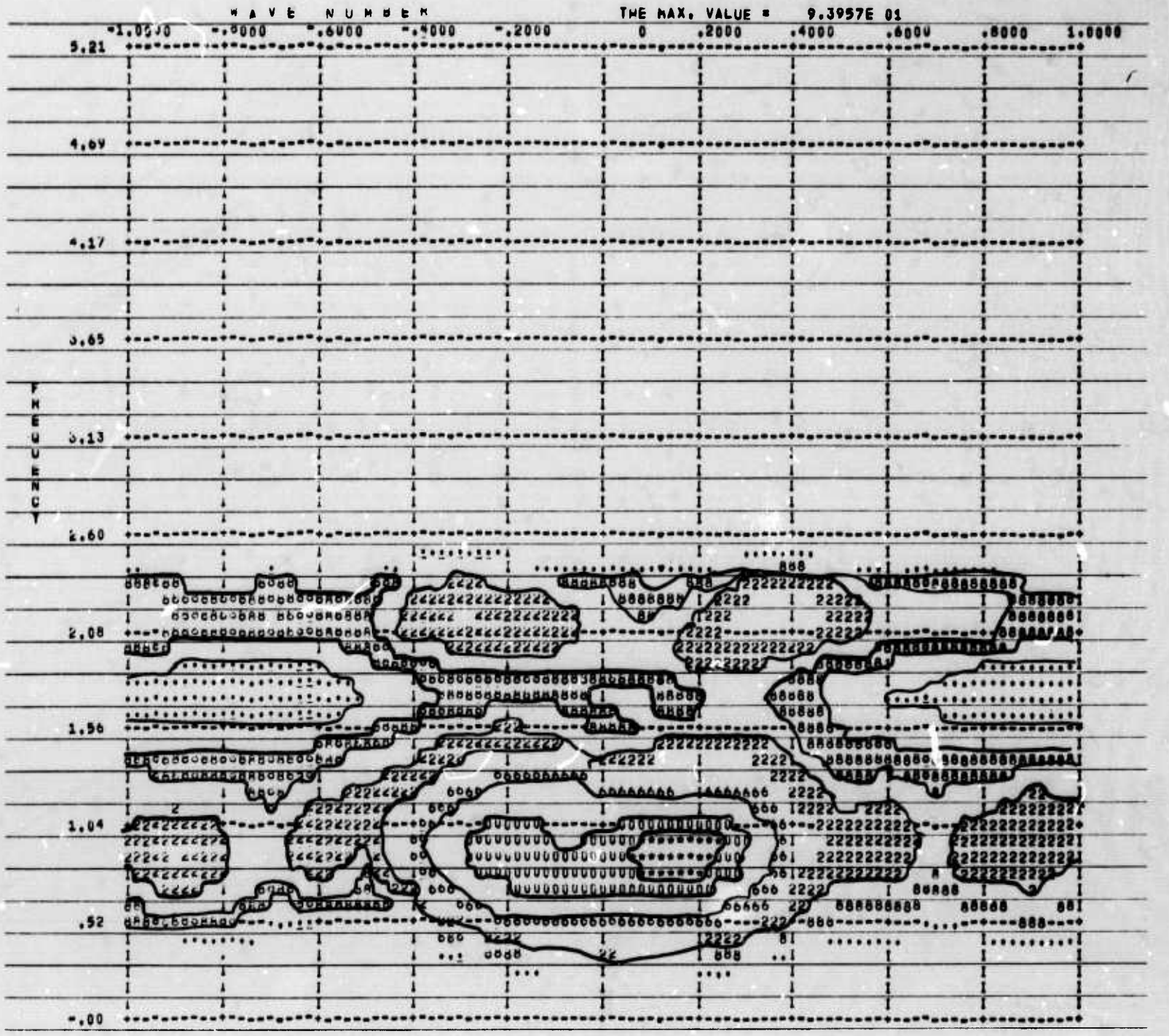

Figure 38. Frequency wave number analysis with noise present for Fiji Island event.

Unclassified
Security Classification

DOCUMENT CONTROL DATA · R&D

(Security classification of title, body of abstract and indexing annotation must be entered when the overall report is classified)

1. ORIGINATING ACTIVITY *(Corporate author)*
TELEDYNE INDUSTRIES, INC.
ALEXANDRIA, VIRGINIA

2a. REPORT SECURITY CLASSIFICATION
Unclassified

2b. GROUP

3. REPORT TITLE
FREQUENCY DEPENDENT ESTIMATION AND DETECTION FOR SEISMIC ARRAYS

4. DESCRIPTIVE NOTES *(Type of report and inclusive dates)*
Scientific

5. AUTHOR(S) *(Last name, first name, initial)*
Shumway, R.H., George Washington University (Consultant to Seismic Data Laboratory)
Husted, H.L.

6. REPORT DATE
9 January 1970

7a. TOTAL NO. OF PAGES
84

7b. NO. OF REFS
10

8a. CONTRACT OR GRANT NO.
F33657-69-C-0913-PZ01

b. PROJECT NO.
VELA T/9706

c.
ARPA Order No. 624

d. ARPA Program Code No. 9F10

9a. ORIGINATOR'S REPORT NUMBER(S)
242

9b. OTHER REPORT NO(S) *(Any other numbers that may be assigned this report)*

10. AVAILABILITY/LIMITATION NOTICES
This document is subject to special export controls and each transmittal to foreign governments or foreign nationals may be made only with prior approval of Chief, AFTAC.

11. SUPPLEMENTARY NOTES

12. SPONSORING MILITARY ACTIVITY
ADVANCED RESEARCH PROJECTS AGENCY
NUCLEAR MONITORING RESEARCH OFFICE
WASHINGTON, D.C.

13. ABSTRACT

A frequency dependent detection and estimation procedure based on the generalized likelihood principle is applied to several models appropriate for vertical and horizontal seismic arrays. When data is constructed so as to conform to the idealized model excellent agreement with theoretical detection limits is shown. Multiple signal models are analyzed in the frequency domain with the presence of various signal components indicated in terms of power spectral ratios. Table of the central and non-central F distribution are used to determine false alarm and signal detection probabilities. A number of examples using real seismic data are presented.

14. KEY WORDS
Arrays
Seismic Detection
Statistical
Maximum Likelihood
Filter

Unclassified
Security Classification